A SIMPLIFIED APPROACH TO THE OPTIMIZATION OF STAINLESS STEEL HONEYCOMB SANDWICH IN COMPRESSION

By

WILLIAM CROMER BURKITT

Bachelor of Science
University of Tulsa
Tulsa, Oklahoma
1948

Submitted to the Faculty of the Graduate School of
the Oklahoma State University
in partial fulfillment of the requirements
for the degree of
MASTER OF SCIENCE
May, 1960

A SIMPLIFIED APPROACH TO THE OPTIMIZATION OF STAINLESS STEEL HONEYCOMB SANDWICH IN COMPRESSION

Thesis Approved

Roger L. Flanders.
Thesis Adviser

Dean of the Graduate School

PREFACE

In August of 1958 Douglas Aircraft Company allotted man-hours and money for the purpose of developing design and construction capability within the company, in the use of stainless steel honeycomb sandwich. I was one of a group of stress analysts at the Tulsa Division, assigned to study the problems of stress analysis as applied to sandwich structures.

In an attempt to catch up with the rapidly changing state of the art, the group undertook a literature survey, in conjunction with similar groups from the Design and Process sections.

We ordered, and received, tons of material. Government publications, manufacturers' reports, research papers, magazine tear sheets, books, all were funneled to the appropriate groups, and read, re-read, digested, and evaluated.

In the field of stress analysis, several interesting facts became apparent. On the one hand, quite a bit of test data was found in many scattered places. On the other hand, a good deal of purely theoretical work was being done by a number of investigators. Only a small part of the literature was found to be concerned with comparing the data to the theories. The reduction of theory to usable form, and the correlation of data became a large part of the group effort.

A surprising fact which came to light, was that the subject was so new that no attempt had been made to cover the field, or any one part of the field. No introductory material defining concepts,

physical properties, or modes of failure, or attempting to relate the findings of different investigators, was available. Our study was therefore a 'bootstrap' operation of self-education.

One of the normal functions of the Strength Group is the evaluation of the load-carrying structure designed by other groups. Accordingly, I was assigned the problem of evaluating methods of selecting efficient configurations of sandwich structure.

Finding little on the subject, and that little difficult to interpret, I began to attempt an independent approach to the problem. I shortly found a device, apparently overlooked by other investigators, which reduced the problem to the study of a three-dimensional surface. However, the equation of the surface was quite complex, and the necessary calculations were extremely laborious. Much credit is due my supervisor, R. L. Keirsey, for encouragement, criticism, and assistance in this labor.

When the allotted time and money ran out, we reported our findings, including the bare idea of the new optimization procedure, in Engineering Report TU-24440. The group was broken up and the members returned to their usual duties.

Some time previously, I had begun Extension courses at Oklahoma State University, and had come under the influence of Professor Jan J. Tuma, who expressed interest in the work described above. At his suggestion I prepared a report for seminar credit, which attempted to fill the need for a correlation between test data and theory, and provide some background in terms of explanation of concepts and modes of failure, for the engineer unfamiliar with honeycomb construction.

He further accepted the suggestion that if the optimization

procedure described above, could be developed into practical form, it might be a suitable subject for a Master's thesis.

Since that time, I have spent many working hours, as time permitted, and many more on my own time, increasing my own understanding of the problem, and evolving methods of simplifying the calculations required. The present form requires less calculation, and provides more insight into the physical problem, than any I have been able to find in the literature.

Grateful acknowledgment is due the Douglas Aircraft Company for the scholarship monies I have received, the library, and other facilities I have used, and the associations I have used to advantage, in the preparation of this paper. It is my hope that its publication will repay, in some small part, my indebtedness to the Company.

Acknowledgment is also due my thesis adviser, Professor R. L. Flanders, for his help and advice in the preparation of this paper.

TABLE OF CONTENTS

Chapter — Page

I. INTRODUCTION AND BACKGROUND 1

Introduction 1
Limitations and Scope 4
Panel Physical Properties and Related Characteristics. 5
Core Density 5
Apparent Core Extensional Modulus 8
Apparent Core Shear Modulus 8
Shear Instability 13
Edge Fixity Considerations. 14
Plasticity Considerations 16
Material Properties 19

II. MODES OF FAILURE 21

Introduction 21
Column Buckling 21
Panel Buckling 22
Monocell Buckling 26
Wrinkling. 28

III. THE OPTIMIZATION PROBLEM. 30

Review of Previous Investigations. 30
A Simplified Approach. 32
Numerical Calculations 37
The Use of Figure 11 48
Summary and Conclusions. 51

REFERENCES. 55

APPENDIX A. 58

Introduction 58
Partial Differentiation With Respect to Structural Index 58
Partial Differentiation With Respect to Stress 59
List of Symbols. 65

LIST OF TABLES

Table — Page

I. Solutions of Equations (6) and (8) for 17-7PH TH1050 39

II. Solutions of Equations (6) and (8) for Optimum Stress and Constant E, 17-7PH TH1050 40

III. Solutions of Equation (7) for 17-7PH TH1050 41

IV. Solution of Left-Hand Side of Equation (A2) 62

V. Solution of Right-Hand Side of Equation (A2). 63

LIST OF FIGURES

Figure		Page
1.	Typical Sandwich Construction	6
2.	Typical Honeycomb Core Configurations	7
3.	Predicted and Measured Core Densities	9
4.	Effective Core Shear Modulus	12
5.	Reduced Moduli For Panel Buckling	18
6.	Tangent and Reduced Moduli For 17-7PH TH1050	20
7.	Predicted and Measured Column Buckling Stress	23
8.	Buckled Panels With Simply Supported Edges	25
9.	Predicted and Measured Monocell Buckling Stress	27
10.	Predicted Wrinkling Stress	29
11.	Design Chart For Panels	42
12.	Efficiency Index Vs. Structural Index	43
13.	Efficiency Index Vs. Stress Level	44
14.	Right-Hand Side of Equation (A2)	64

CHAPTER I

INTRODUCTION AND BACKGROUND

Although various kinds of material sandwiches have seen varied uses, usually non-structural, since 1919, and a theory of sandwich behavior was being developed as far back as 1940 (Ref.1), the subject of aircraft use of honeycomb sandwich, particularly metallic honeycomb sandwich, is so new as to have no history.

Airplanes such as the British De Havilland 'Mosquito' of late World War II vintage used a plywood-balsa sandwich construction to advantage, but airplanes using metallic honeycomb sandwich as primary structure, such as the Convair B-70 'Hustler', are being built at the present writing. No such airplanes are old enough that their degree of excellence in terms of cost, performance, and efficiency, can be evaluated with any historical perspective.

However a relative estimate of excellence in terms of performance may be inferred from the wide and growing use of metallic, particularly stainless steel, honeycomb sandwich in the design of current aircraft.

If aircraft, including missiles, can be built any other way, and meet their design requirements, they will be built that other way. Metallic honeycomb sandwich is fantastically expensive, inordinately difficult to fabricate, inspect, and repair, and difficult to design for and analyze. That it is used at all, is a clear indication that this material is the best, and possibly the only available solution to

certain mission requirements. This fact necessarily relegates considerations of cost to the status of 'someone else's problem' as far as the aircraft designer is concerned.

However the fundamental problem of all aircraft structural design, that of designing the lightest possible structure which will carry the design loads, without protruding from the aircraft contour or cluttering up its interior, is even more pressing and difficult than with conventional structure. There is a vast body of experience and theory which may be drawn upon to guide the designer to the optimum configuration of the several conventional types of structure. In contrast, a really useful guide or procedure to aid in the selection of an optimum configuration of stainless steel sandwich structure, does not exist today. In fact the useful guides to selection of even the best 'building block' of such a structure can be numbered on the fingers of one hand. (See References 1 through 4)

By 'building block' is meant the fundamental load-carrying element of structure. Because of the inherent instability of lightweight structure, the most difficult single problem of the aircraft structural designer is the design of efficient compression structure. In conventional compression structure as exemplified by wing spar caps and stringers, fuselage longerons, and landing gear linkage, the fundamental load-carrying element is the classical Euler column, complicated by considerations of low slenderness ratio and local instability such as flange buckling and crippling. NACA TN 2435 (Ref.5) gives direct-reading design charts for aluminum alloy sheet-and-stringer composite columns, enabling the designer to select the optimum configuration of this common type of wing construction methodically and rapidly. (Gerard (Ref. 6)

Chapter 3) gives typical experience and trend data to enable the designer to consider the effects of such parameters as wing rib weight, and to integrate these effects into the selection of sheet-and-stringer combinations so as to optimize the structural weight of the entire wing.

In contrast, because of the higher inherent stability of honeycomb sandwich, the 'building block' of this type of structure is the classical panel, complicated also by local instability, such as wrinkling and dimpling, and by 'shear instability' due to the flexibility of the honeycomb core.

As is generally known, the load-carrying capability of a column decreases as the second power of increasing column length. In contrast, as will be shown later, the load-carrying capability of a panel in compression decreases as the second power of increasing panel width. Thus in the typical case of an airplane wing, which functions basically as a cantilever beam, conventional structure dictates many ribs to shorten the effective column length of spar caps and stringers, while sandwich structure requires relatively more spars to decrease individual panel width, and fewer ribs since panel length is an unimportant parameter. This fact weakens, not to say invalidates, such otherwise excellent procedures and parameter studies as Reference 6 for application to sandwich structures.

Finally, as noted above, little useful help is available in the literature to the designer as he seeks to optimize his fundamental 'building block', the classical panel, modified to the practical stainless steel honeycomb sandwich panel. It is the purpose of the present paper to investigate this problem, comment on the existing literature,

and propose a solution which appears to have practical advantages over previous ones.

Limitations and Scope

Before proceeding further, it appears desirable to attempt some definition and limitation of scope. In the first place, several types of honeycomb sandwich are available, differing widely in properties, method of fabrication, and price. Sandwich panels are fabricated from kraft paper, wood veneer, fibreglass, dural, titanium, and several stainless steels, to name the most common materials. Assembly is accomplished by glueing, organic bonding, brazing, resistance welding, and solid-state (pressure) welding, among the more common processes. Obviously a paper of this length cannot adequately cover a field of such magnitude, although many of the principles used are generally applicable.

The scope of this paper, then, is limited to honeycomb sandwich panels suitable for high temperature applications; which eliminates materials other than titanium and stainless steel, and fabrication techniques other than brazing and welding. In particular, the data adduced and sample calculations given, will apply to panels fabricated by brazing and made from a stainless steel alloy, 17-7PH TH 1050, indicating 17% chromium, 7% nickel, and a trace of phosphorus; drawn to a temperature of 1050 F. after cooling from brazing temperature.

The only loading condition considered is edgewise compression, and only appropriate modes of failure are considered.

A large number of physical properties of such a panel are of interest, and both theoretical and test values can be found for most of

these in the literature. However, for the purposes of this paper, some properties will be dealt with rather cursorily, while others will receive a fairly full treatment.

Panel Physical Properties and Related Characteristics

One of the fundamental assumptions of most structural analysis, along with Hooke's Law and small deflections, is homogeniety of material. Since any sandwich is by definition not homogeneous, the structural analysis of homeycomb sandwich contains terms and concepts not found in other such analysis. Most of these terms describe properties of the honeycomb core itself. The construction of a typical sandwich is shown in Fig. 1, along with the symbols used to denote significant dimensions. The symbols are those of ANC-23 Part II(Ref.7) except where those were found to be inadequate. A complete list of symbols is given on page 65.

Core density d_c. The fundamental honeycomb core parameter is the weight density, usually given in pounds per cubic foot (pcf). This is not primarily because the weight is significant, but because all the other important core parameters can be estimated from it. The density itself can be estimated with good accuracy from the cell size and shape, and the thickness of the steel foil or ribbon from which the core is made. Practical steel core densities range from 5 to 25 pcf. Since the density of 17-7 PH stainless steel is approximately 477 pcf, the advertising boast of honeycomb manufacturers that their product is 97% air, is not exaggerated.

Figure 2 shows the regular hexagonal shape favored by some honeycomb manufacturers, the slightly modified square used by others, and the idealized square used for simplified analysis of square cell honeycomb.

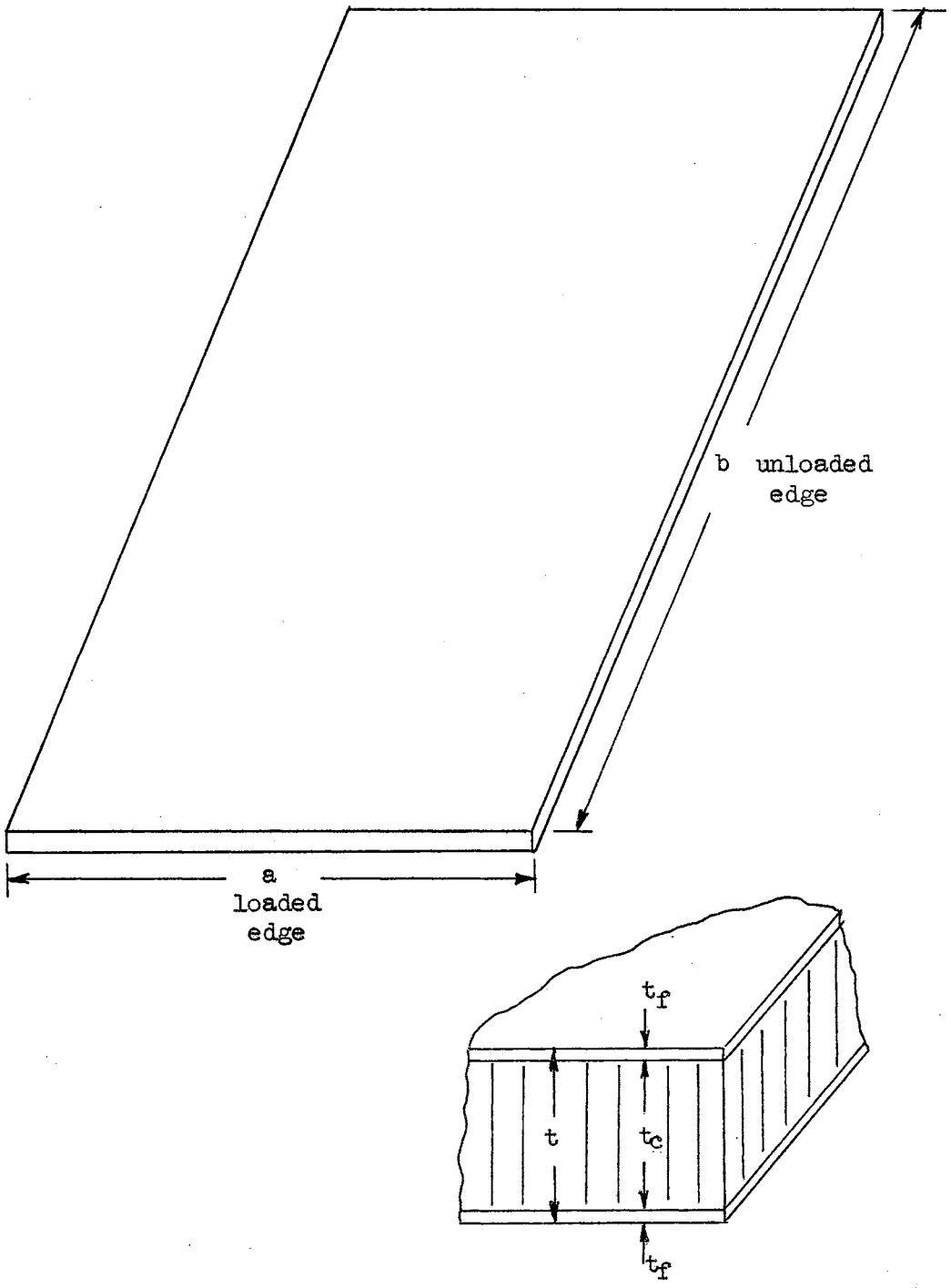

Figure 1. Typical Sandwich Construction and Panel Geometry

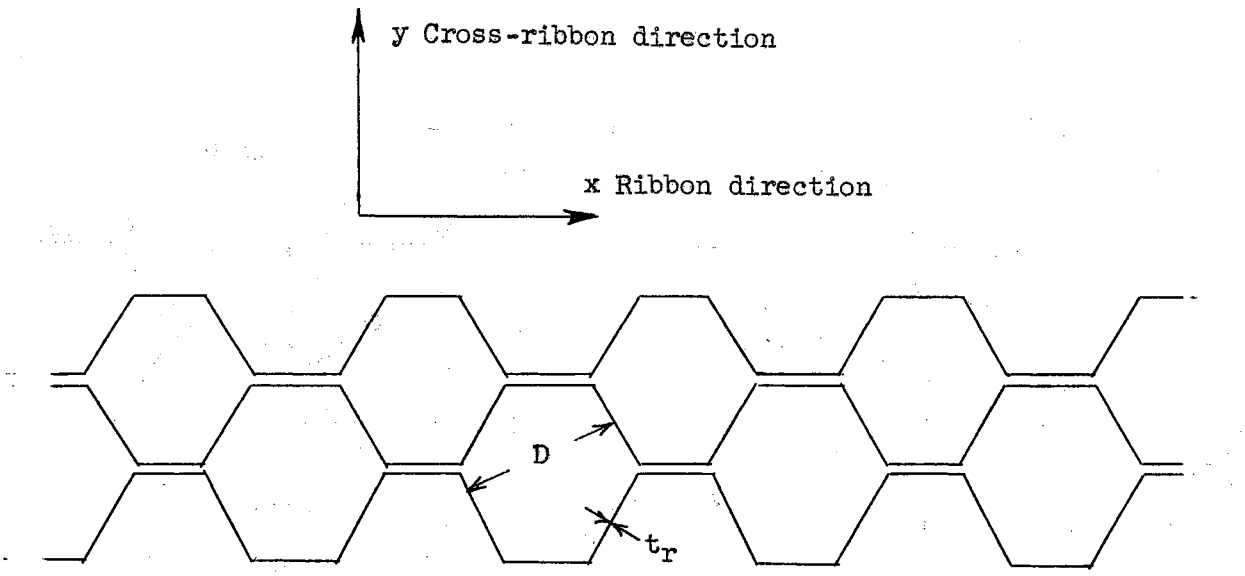

(A) Hexagonal Cell

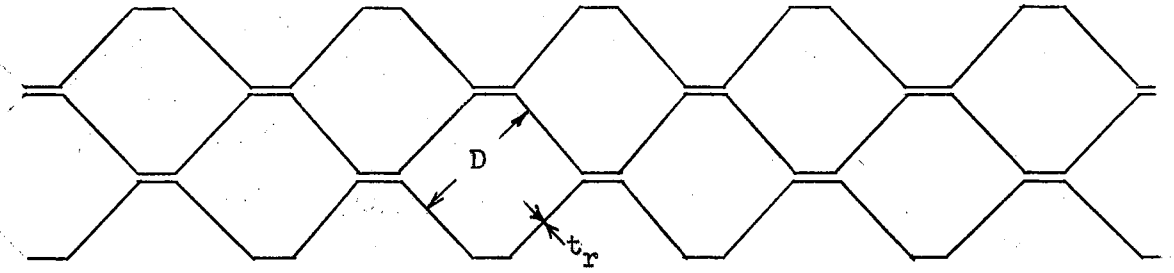

(B) Square Cell

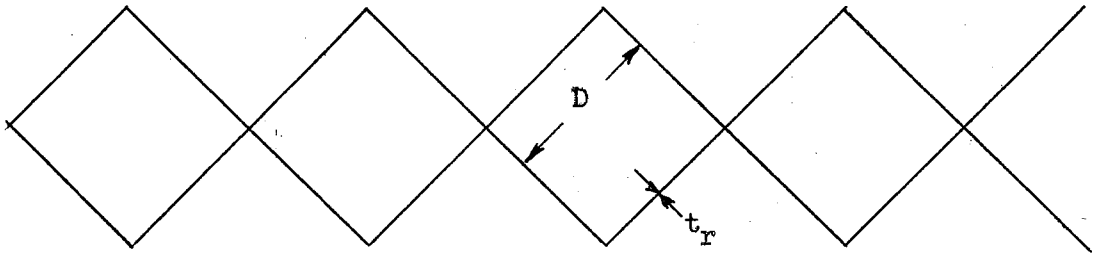

(C) Idealized Square Cell

Figure 2. Typical Honeycomb Core Configurations

From a consideration of the percentage of the total volume of the honeycomb occupied by metal, it is rather easy to derive expressions for the core density in terms of cell size 'D' and ribbon gauge 't_r' (Appendix A of Ref. 1). These expressions are:

$d_c = 8/3\ (t_r/D)477$ for hexagonal cells

$d_c = 2\ (t_r/D)477$ for idealized square cells

$d_c = 2.22(t_r/D)477$ for practical square cells

The usefulness of these expressions is indicated in Fig. 3 where measured core densities from various sources are compared to the predicted values.

Apparent core extensional modulus E_{zc}. This is a little used and rarely measured parameter. It is the out-of-plane stiffness of the core and obviously can be predicted by multiplying the percentage of steel in the honeycomb by the Young's modulus of the steel. Using the results of the preceding paragraph:

$E_{zc} = 8/3\ (t_r/D)\ E$ for hexagonal cells

$E_{zc} = 2\ (\ t_r/D)\ E$ for square cells

Certain theories of face wrinkling (see page 28) consider the sandwich faces as columns supported on a continuous elastic medium. The elastic properties of this medium (the honeycomb core) are obviously essential to the development of the theory.

Apparent core shear modulus G_c, G_{cxz}, G_{cyz}. In the development of sandwich panel theory, the assumptions are made that the honeycomb core can be treated as a material with 'apparent' physical properties and that it will resist all loads acting out of the plane of the panel. That is, all edgewise loads such as tension, compression, and 'picture frame' shear, are carried entirely by the two faces, while loads applied

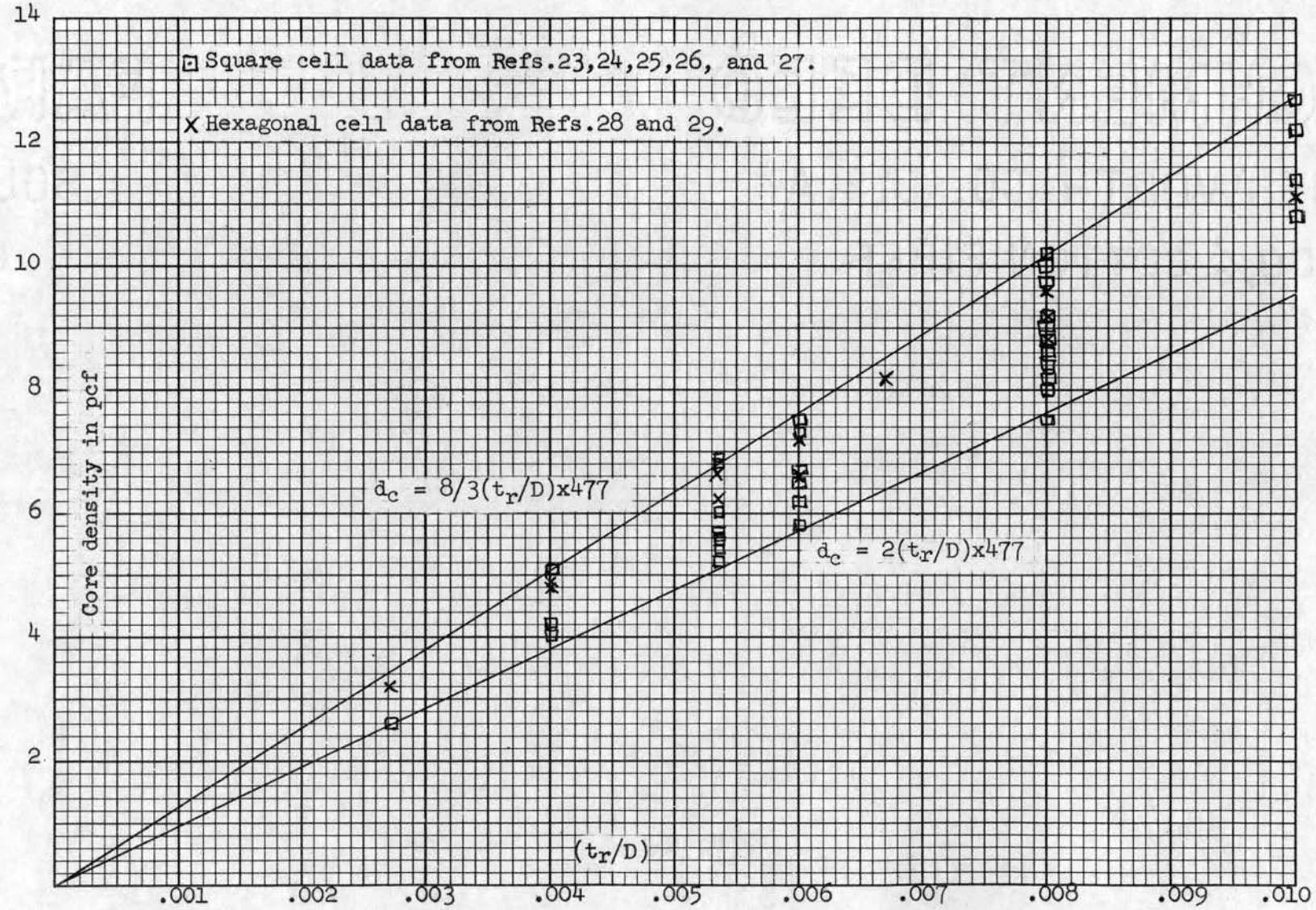

Figure 3. Comparison of Predicted and Measured Honeycomb Core Densities. 17-7PH

normal to the faces of the panel produce bending in two directions, which is reacted by axial loads in the faces, and shear which is carried entirely by the core. The strain in the core is significant under rather small shear stresses, and cannot be neglected as an energy-storing mechanism. This is in contrast to usual analysis assumptions in which bending is reacted by a stress distribution which varies linearly from the outermost fibre to the neutral axis, and shear strain is considered negligible.

Thus the apparent shear modulus of a honeycomb core is the shear modulus of an hypothetical homogeneous material which occupies the same space as the core, and strains in shear at the same rate.

However it is important to note that this hypothetical material while homogeneous, is not necessarily isotropic. It is apparent from Fig. 2(A) that more material in each hexagonal cell is oriented in the ribbon direction than normal to it. Intuition suggests that the core should be stiffer in shear along the ribbon (G_{cxz}), than in the direction normal to the ribbon (G_{cyz}). Thus a hexagonal honeycomb core is orthotropic; that is, it has different material properties along mutually perpendicular axes.

A core of idealized square cell honeycomb can be shown to have equal lengths of ribbon oriented along the ribbon direction, normal to it, and in all directions in between. Thus a square cell honeycomb core is effectively isotropic.

Because panel formulas for isotropic materials are much simpler than those for orthotropic materials, a considerable computational advantage is gained by using the 'effective' apparent core shear modulus (G_c) expression given by Kaechele in Appendix A of Ref. 1. This gives a

sort of average apparent core shear modulus for orthotropic cores, which may be used in isotropic formulas. It is $G_c = \frac{2G_{cxz}G_{cyz}}{G_{cxz} + G_{cyz}}$.

Reference 8 is by far the most comprehensive and thorough discussion of core shear moduli in the literature. The results of this discussion lead, in part, to the following conclusions:

for hexagonal cells $3/2\ (t_r/D)G < G_{cxz} < 5/3\ (t_r/D)G$ or

$$G_{cxz} \approx 19/12\ (t_r/D)G$$

and $$G_{cyz} = (t_r/D)G$$

where G is the shear modulus (modulus of rigidity) of the material from which honeycomb is made. Applying the approximation above,

$$G_c = \frac{2G_{cxz}G_{cyz}}{G_{cxz} + G_{cyz}} = \frac{2(19/12)x\ 1}{(19/12)+ 1}\ (t_r/D)G = (38/31)(t_r/D)G$$

For square cell honeycomb

$G_c = (t_r/D)G$

Combining these results with those of the section on core density, and taking $G = 11.5 \times 10^6$ for steel,

$G_{cxz} = (19/12)(t_r/D)G = (19/12)(3/8)(d_c/477) \times 11.5 \times 10^6 = 14300\ d_c$

$G_{cyz} = (t_r/D)G = (3/8)(d_c/477) \times 11.5 \times 10^6 = 9000\ d_c$

$G_c = (38/31)(t_r/D)G = (38/31)(3/8)(d_c/477) \times 11.5 \times 10 = 11080\ d_c$

for hexagonal cell core; and for square cell core,

$G_c = (t_r/D)G = (1/2.22)(d_c/477) \times 11.5 \times 10^6 = 10850\ d_c$

These relationships are plotted in Fig. 4 with some data from Reference 8 indicating acceptable agreement between theory and test data. It is noteworthy that there is less than 2% difference between the hexagonal and square expressions for G_c, which is well within the limits of experimental error. For simplicity and conservatism it is hereinafter assumed that $G_c = 10000\ d_c$ is sufficiently accurate for any practical

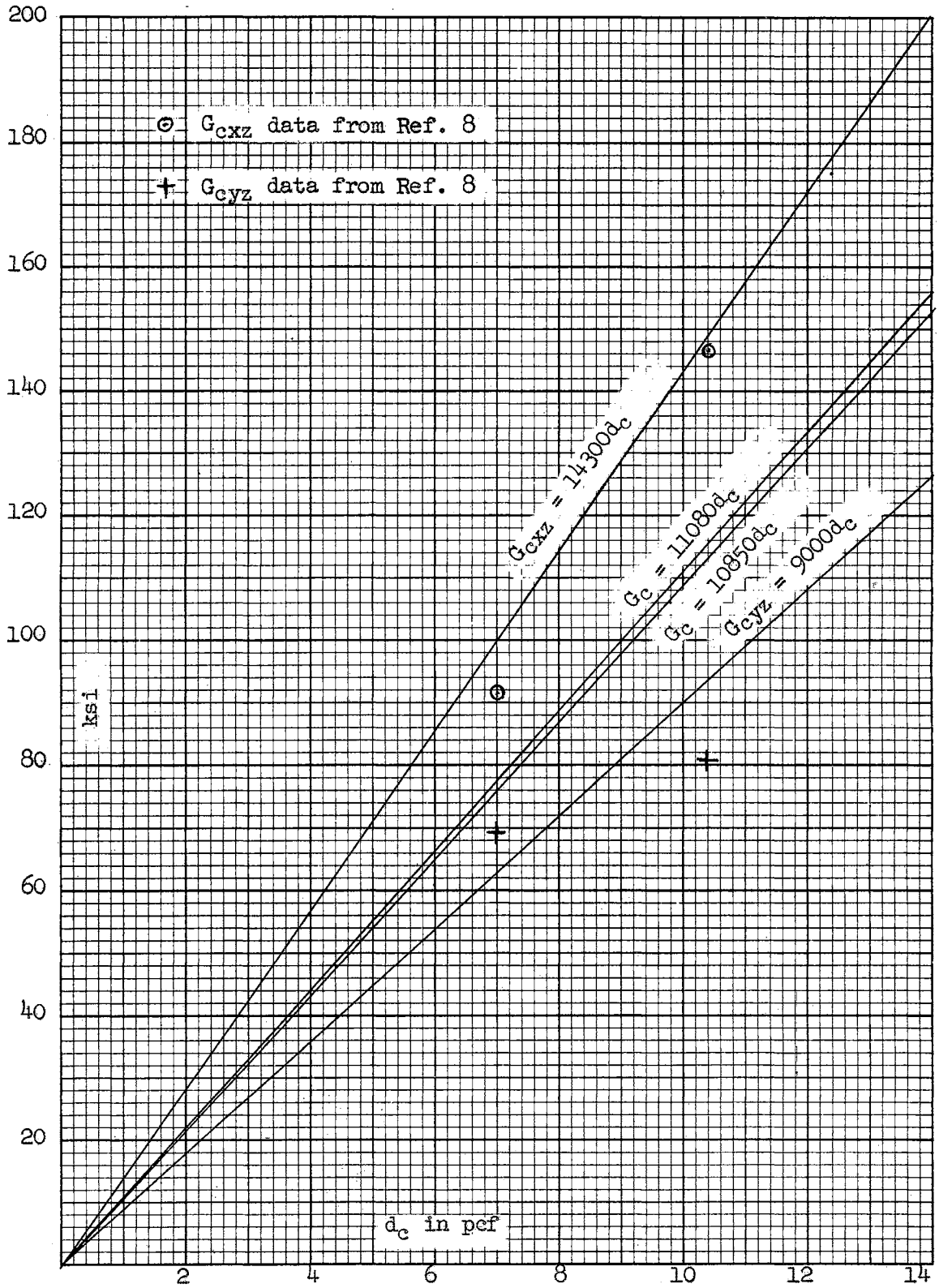

Figure 4. Effective Core Shear Modulus vs. Core Density for 17-7PH

honeycomb core configuration made from 17-7PH TH 1050.

Shear instability This is a term describing the influence of the shear deflection of the core on the behavior of a sandwich panel under load. It may best be visualized by considering the effect of core shear deflection on the stability of a sandwich column. A relatively long slender column ($L'/\rho > 20$ for sandwich) is assumed, with the ends ground square. Such a column will behave in a test fixture as a fixed-ended column.

As load is applied the usual unavoidable small eccentricity causes a slight curvature to develop. This curvature causes bending moments which tend to increase the curvature. This is normal (Euler) column instability. Due to the fixity developed by the flat square ends, points of inflection (zero moment) will appear approximately at the upper and lower quarter-length points.

Since the bending moment varies from a maximum at the mid-point to zero at the quarter-length points, obviously a beamwise shear is acting across the column, equal to the rate of change of the bending moment. The moment is changing from positive to negative at the two points of inflection so that maximum shear occurs at these points.

This shear produces shear deflection in the honeycomb core which contributes to the offset at the midpoint of the column, which increases the bending moment, which increases the shear, producing more offset, so that the column is actually more unstable than indicated by the Euler formula, and fails at a lower load. If the core is fairly light, obvious shear damage in the core at the quarter-length points, will accompany the failure.

The picture is similar but more complicated in the panel case, in

that panel buckling produces bending and hence core shear, in two directions (along and across the ribbon). It is still intuitively apparent however, that the shear flexibility of the honeycomb core contributes to the overall instability of the panel in compression (and also in panel shear). An extreme case can be imagined in which shear deflection of the core so far outweighs bending deflection of the panel that collapse occurs before much bending can be developed. This is the significance of 'shear instability'.

Edge fixity considerations In the column case (page 21) shear instability is handled by an additional term. In the case of the panel it is conveniently considered as modifying the panel buckling coefficient 'K', which also describes the effect of the edge support conditions.

For a given set of edge conditions, say all edges fixed, or two edges fixed, K is a complex function of the aspect ratio (b/a) of the panel, and the parameter 'V', which is a dimensionless ratio of the panel bending stiffness to the shear stiffness.

For the particular case of all four edges simply supported, and aspect ratio greater than about three, the relationship simplifies to $K = \frac{4}{(1+V)^2}$ (Ref.9, Eq.2). Since the corresponding value for a homogeneous panel is K = 4 (Ref. 10, Table 7), the correction for shear instability is clearly apparent. Furthermore, since for homogeneous materials the assumption of infinite shear stiffness is usually made (i.e. V = 0), the correction is clearly in the right direction.

As noted previously, honeycomb sandwich is usually employed as a panel or a group of contiguous panels formed by subdividing a large panel by crossing substructure such as wing ribs and spars. The edge

support conditions which may reasonably be assumed for such panels obviously depend on the substructure. If this structure is just stiff enough to hold all four edges of each panel straight but to permit them to roll, so that each downward buckle in a panel is adjacent to an upward buckle either in the same panel or across a support line in the surrounding panels (checkerboard pattern), the classical case of simple support may be assumed. If, due to stiffer support structure, or initial curvature, or normal loading, the panels tend to buckle symmetrically about each support line, then the condition of fully fixed edges is approached. The situation is exactly analogous to conventional wing structure consisting of axially loaded stringers lying across regularly spaced ribs. Obviously any one stringer can bow upward between two ribs, and downward in the adjacent bays inboard and outboard. Since rotation occurs at each rib, it is reasonable to analyze each bay as though the stringers have pinned ends at each rib. This is somewhat conservative but is standard practice in some aircraft companies. Other companies assume some slight degree of end fixity at each rib, as a result of experience.

It therefore seems reasonable to suppose that as experience is gained in the design of structures using honeycomb sandwich panels, some experience factor for edge fixity will evolve. However such experience is meager today and also proprietary. The published literature is inadequate to support any assumption other than simply supported edges. As noted in Reference 1, page 3, the major theories of panel buckling reduce to a common result for the case of simply supported edges which also offers significant computational advantages over other conditions, as described above. For the purposes of this study then, panels will be

assumed simply supported on all four edges. See Fig. 8.

Plasticity considerations In order to realize satisfactory efficiency from stainless steel in aircraft construction, it is necessary to stress it far above the proportional limit. The utility of honeycomb construction rests on its ability to stabilize steel sheets to the extent that they can withstand such high stresses in compression and shear. However nearly all structural analysis is predicated upon the applicability of Hooke's law that strain is proportional to stress. By definition this law does not apply above the proportional limit of stress.

The problem is not acute for most common materials for which the yield point and proportional limit are close together, and about two-thirds of the ultimate strength. For aircraft aluminum alloys and stainless steels, which have no well-defined yield point, the stress at which a line of slope E, offset .2% strain, intersects the stress-strain curve, is arbitrarily defined as the yield stress. On this basis the typical stainless steel 17-7PH TH1050 has a proportional limit of 93,000 psi, a yield stress of 185,000 psi, and an ultimate strength of 200,000 psi (Reference 11). It is apparent that the useful range of stress levels for this material is entirely in the plastic range. The problem of plastic behavior must be considered for such materials.

The neatest device for considering stresses in the plastic range is the so-called 'reduced' modulus. This is simply an attempt to relate the plastic behavior of a material, in a particular mode of failure, to the non-linear part of its stress-strain diagram, just as the Young's modulus relates elastic behavior to the straight-line portion.

Stowell in NACA Report No. 898 (Ref. 12) has developed a unified

theory of elastic and plastic buckling of panels which considers column buckling as a limiting case. His results indicate various complicated functions of the stress-strain diagram as suitable reduced moduli for different conditions of edge restraint, including the use of the tangent modulus for column buckling. This agrees with the work done by other investigators (Ref. 10). Seide and Stowell in NACA Rep. 967 (Ref. 9) have applied Stowell's theory to sandwich (not honeycomb) panels with fair test agreement, but the results reflect the effects of panel geometry as well as the material stress-strain diagram, and hence do not permit expression in terms of a simple reduced modulus.

By a process of back-figuring from Reference 9 the curves of Fig. 5 have been prepared, indicating that the effects of practical ranges of panel geometry are relatively small and for a parameter study such as this paper, may be neglected. On the basis of Fig. 5 a reduced modulus of $E_R = \frac{4EE_t}{(\sqrt{E}+\sqrt{E_t})^2}$ has been selected for panel buckling, although the use of any other reduced modulus will not significantly affect the analysis of panel buckling. For column buckling the same reduced modulus is arbitrarily assumed. For wrinkling and monocell buckling the tangent modulus has been used simply because it appears to give good results.

Another significant effect of stresses above the proportional limit is the change in Poisson's ratio. This material property accounts for the bi-axial stress state in the panel faces. For aluminum and steel this ratio lies between .25 and .33 in the elastic region, but assumes a value of .50 in the fully plastic region (Ref. 10, page 17). In the yield region a transition occurs which is given by equation 25 of Reference 10 as $\mu = \mu_p - (E_s/E)(\mu_p - \mu_e)$ where subscript 'p' refers to

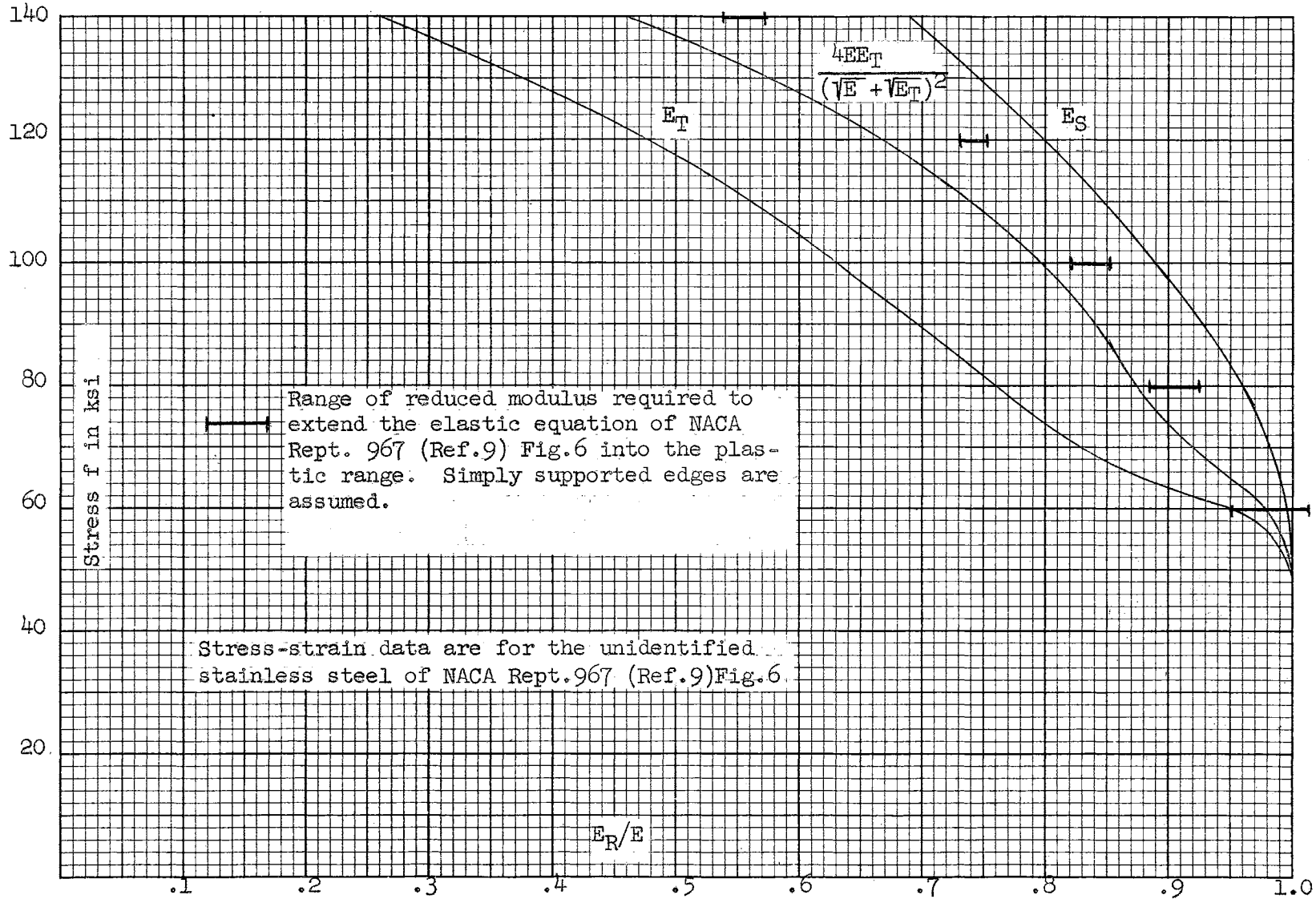

Figure 5. Comparison of Reduced Moduli for Panel Buckling.

fully plastic and subscript 'e' refers to fully elastic. Neglecting this transition, the value $\nu = .50$ is used throughout this paper.

Material properties The density of 17-7 PH TH1050 is given in Reference 13 as .276 lb./cu. in. It is used in this paper as 477 lb./cu. ft. (pcf)

Tangent modulus in compression data for 17-7 PH TH1050 is taken from NACA TN 4074 (Ref. 11) and is presented in figure 6. The 'reduced' modulus E_R, shown in the same figure, is calculated from the E_T curve by means of the expression shown. The derivative of the reduced modulus with respect to stress is simply scaled from the E_R curve.

Significant points on the stress-strain curve are (from Ref. 11)

Proportional limit	93,000 psi
.2% offset yield strength	185,000 psi
Ultimate compressive strength (assumed)	200,000 psi

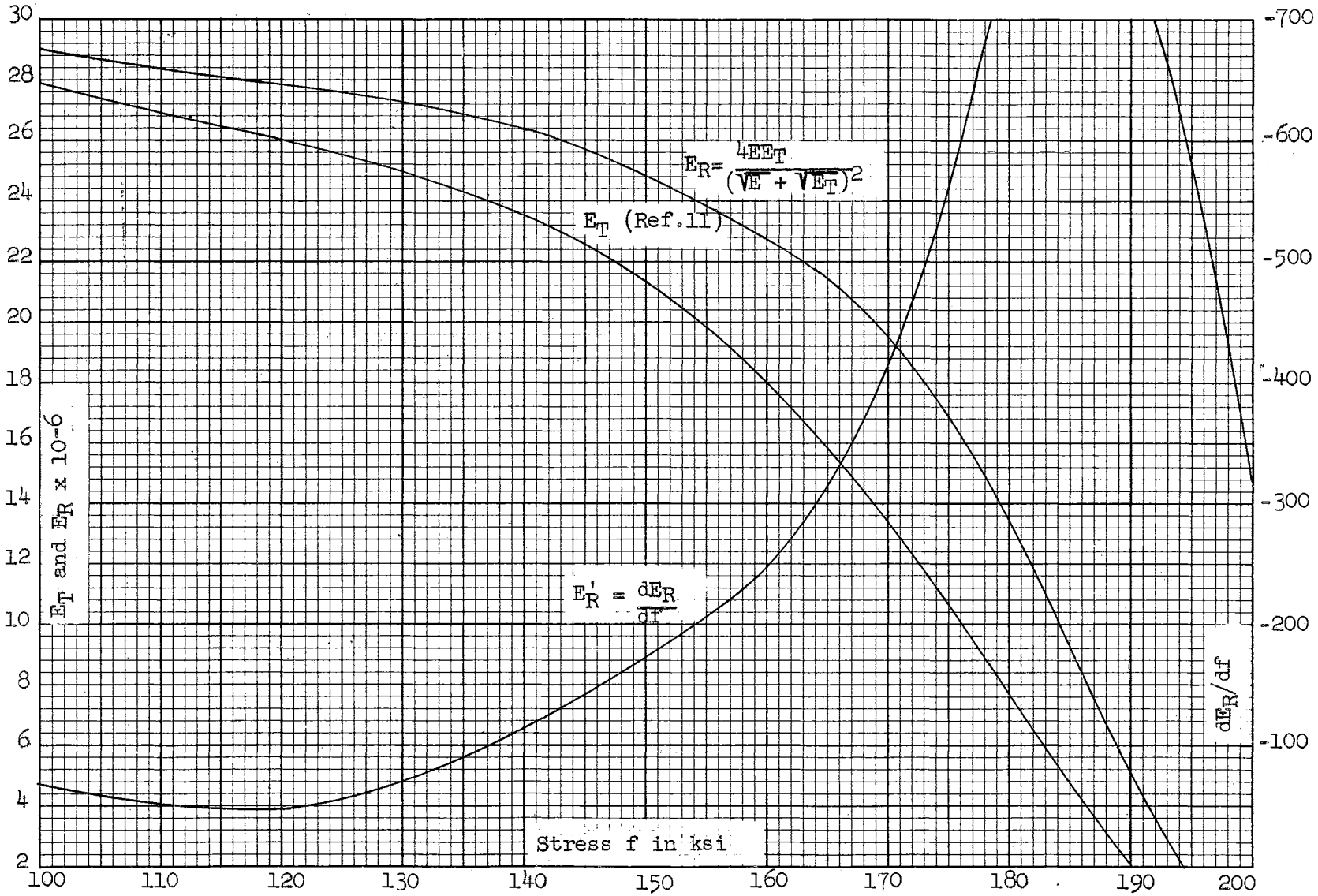

Figure 6. Reduced Modulus in Compression Data for 17-7PH TH 1050

CHAPTER II

MODES OF FAILURE

Honeycomb sandwich can fail in a number of ways, depending to some extent on the manner of loading. Only those which can occur due to edgewise compression will be described in this paper.

Although the panel is the basic structural unit, much testing is done on sandwich columns. For this reason a discussion of column buckling, adjusted for plastic behavior due to high stress level and shear instability due to flexibility of the honeycomb core, is included.

Column buckling The column buckling equation for sandwich is the usual Euler equation with an extra term to account for shear flexibility of the core. It is most concisely written in the form

$$\frac{1}{P_{cr}} = \frac{1}{P_E} + \frac{1}{P_s} \qquad \text{(EQ 1)}$$

where P_{cr} is the critical load, P_E is the critical load if core flexibility is not considered (the Euler critical load), and P_s is the core shear flexibility correction, called in this form, the shear instability load. Among others, Williams in Reference 3 gives this expression.

Making the following substitutions,

column area = $2at_f$
column length = b for a pin-ended column
radius of gyration, = $(t_c + t_f)/2$

$$P_E = \frac{\pi^2 E_R I}{(L)^2}$$

$$P_s = at_c G_c$$

Equation (1) can be re-arranged to give

$$\left(\frac{L}{e}\right)^2 = \left(\frac{2b}{t_c + t_f}\right)^2 = \frac{\pi^2 E_R}{F} - \frac{2\pi^2 t_f E_R}{t_c G_c} \qquad \text{(EQ 2)}$$

This equation is plotted on page 23 for 17-7PH TH 1050 assuming

$$E_R = \frac{4EE_T}{(\sqrt{E} + \sqrt{E_T})^2}$$

Two data points from Reference 14 are shown, indicating fair agreement.

Pertinent values are G_c = 34400 psi
t_c = .313 in.
t_f = .008 in. (point 1)
t_f = .012 in. (point 2)

Panel buckling A general form of the panel buckling equation, given in Reference 4, in the symbols used in this paper, can be written

$$P_{cr} = \frac{K\pi^2 E_R I}{a^2}$$

If the substitutions

$$I = (1/12)at^3$$
cross-sectional area = at

are made for homogeneous panels, there results

$$F = \frac{K\pi^2 E_R}{12}\left(\frac{t}{a}\right)^2$$

If the substitutions

$$I = \frac{2at_f}{\lambda}\left(\frac{t_c + t_f}{a}\right)^2$$
cross-sectional area = $2at_f$

are made for sandwich panels, there results

$$F = \frac{K\pi^2 E_R}{4\lambda}\left(\frac{t_c + t_f}{a}\right)^2$$

For simply supported edges and an aspect ratio greater than three, K is 4 for a homogeneous panel (Ref. 10, Table 7), and $4/(1+V)^2$ for a sandwich panel. (See page 14)

With these substitutions, the following equations result:

$$F = \frac{4\pi^2 E_R}{12\lambda}\left(\frac{t}{a}\right)^2$$ which is the usual textbook form for

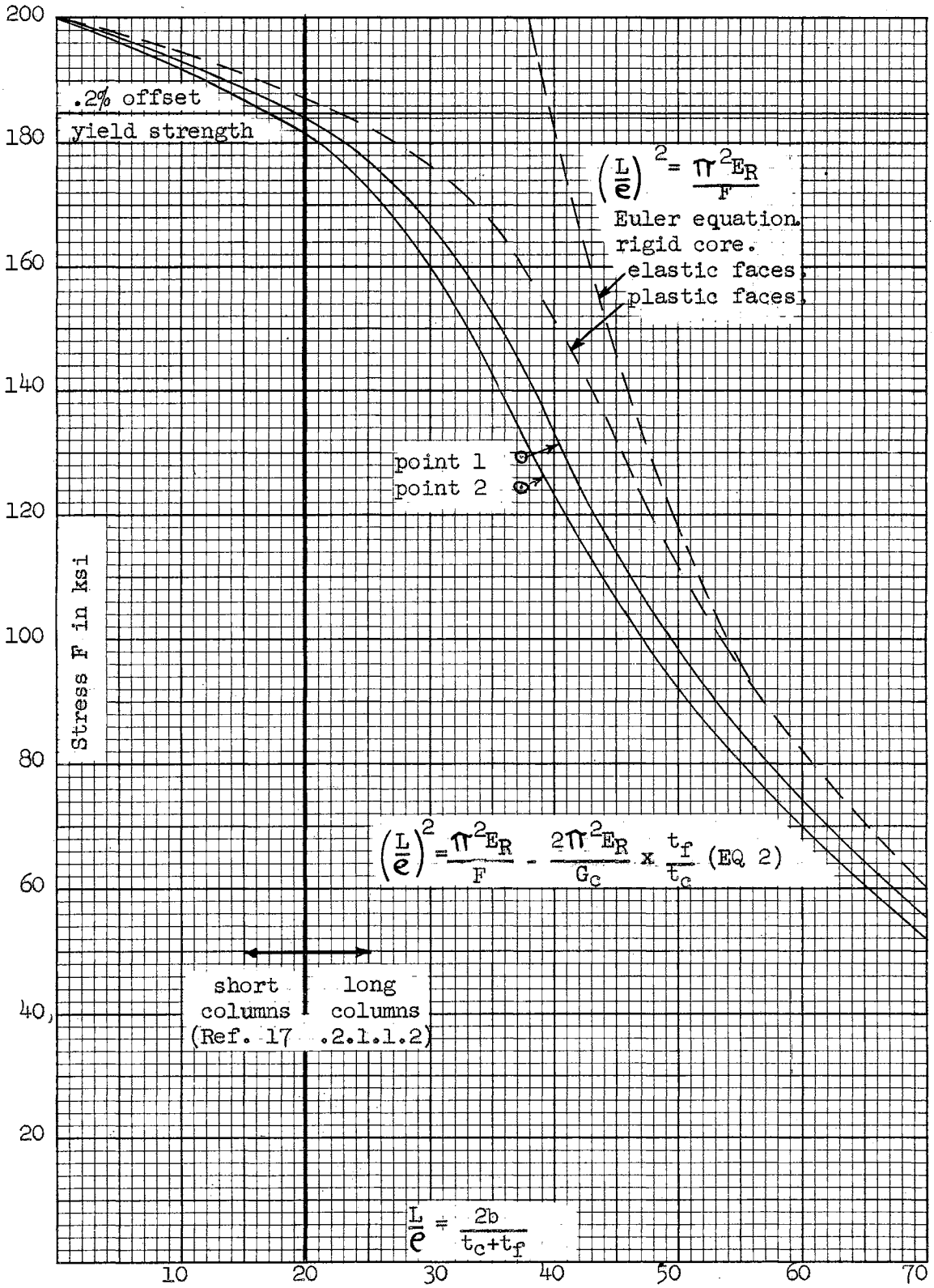

Figure 7. Comparison Between Predicted and Measured Column Buckling Stress for 17-7PH TH1050

homogeneous panels; and

$$F = \frac{K\pi^2 E_R}{4\lambda}\left(\frac{t_c + t_f}{a}\right)^2 \qquad \text{(EQ 3)}$$

which can be obtained from ANC - 23,3.2.1.1 (A) (Ref 7) by substitution. This is the basic equation in the optimization process of this paper, as well as References 1 and 3.

It is of interest to note that the length 'a' of the loaded edge of the panel enters into the panel buckling equation in the same manner as the length 'b' of the unloaded edge enters into the column buckling equation.

It is also instructive to correlate the appearance of a buckled panel (Fig. 8) with the form of Equation 3. The buckled panel will exhibit a wavy deformation pattern in the direction of the load, but only a single half-wave across the panel. This is the reason that the width enters into a 'slenderness ratio' form instead of the length.

Intuitively it might be concluded that little difference in applied stress would be necessary to cause the panel to buckle into, say six, or seven half-waves. This is confirmed by the fact that 'K' becomes a function of V only, for aspect ratios greater than about three, and hence neither the length of the panel nor the number of half-waves enters the equation.

Also intuitively, it might be supposed that a panel with low shear stiffness in the core would buckle at a lower stress than one with a stiff core, and it may be observed in ANC-23 (Ref 7) Fig. 3.1 or in the expression $K = 4/(1+V)^2$, that K, and hence the critical stress decreases with increasing V (decreasing G_c).

A comparison of Eq. (3) with some Boeing Airplane Company data for aluminum honeycomb panels is given in Fig. 8 of Reference 1 and shows

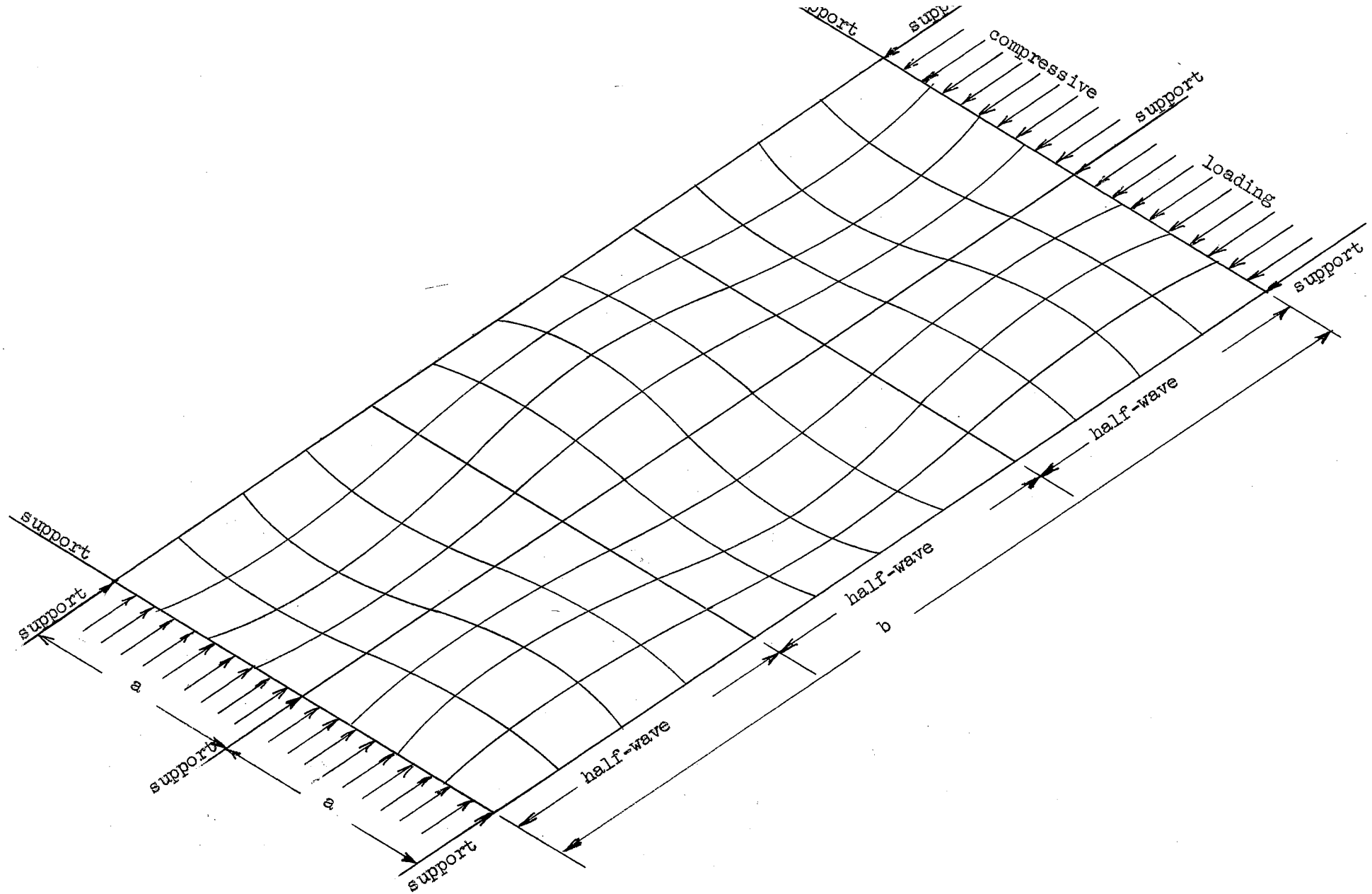

Figure 8. Buckled Panels With Simply Supported Edges.

fair agreement. Somewhat different parameters are used however, and the figure is not suitable for inclusion in this paper.

Monocell buckling In addition to overall instability such as panel and column buckling, edgewise compression of honeycomb sandwich can produce at least two types of local face instability. The simplest of these is monocell buckling, also called 'intracell buckling', 'dimpling', and 'read out'. This occurs when the cell diameter of the core is more than about ten times the thickness of the faces. In this mode of failure the face material buckles locally into each individual cell, producing a 'dimpled' appearance and enabling the honeycomb core configuration to be 'read' through the facing material. Obviously this action depends on the stiffness of the faces and the cell size. The face stiffness depends on the face thickness and the modulus of elasticity.

The relationship between the critical stress and these variables is developed empirically in FPL 1817 (Ref.15) and quoted in ANC-23 (Ref.7). This relationship is

$F = (E_R/3)(t_f/R)^{3/2}$ where R is the radius of the honeycomb cell. In reference 15 the reduced modulus $E_R = \frac{4EE_T}{(\sqrt{E} + \sqrt{E_T})^2}$ is used for aluminum faces with good results. However to be conservative, it is assumed that $E_R = E_T$ for monocell buckling in this paper.

In Fig. 9 the above equation is plotted for 17-7PH TH 1050 and compared to some scattered data from different sources. The significant point about monocell buckling is illustrated in this figure, that is, that at $t_f/R = 20$, the critical stress is very near the yield strength of the material. This is true for many materials, and may be expressed as a rule of thumb that monocell buckling will not be critical as long as the cell size is not more than ten times the face thickness. It is

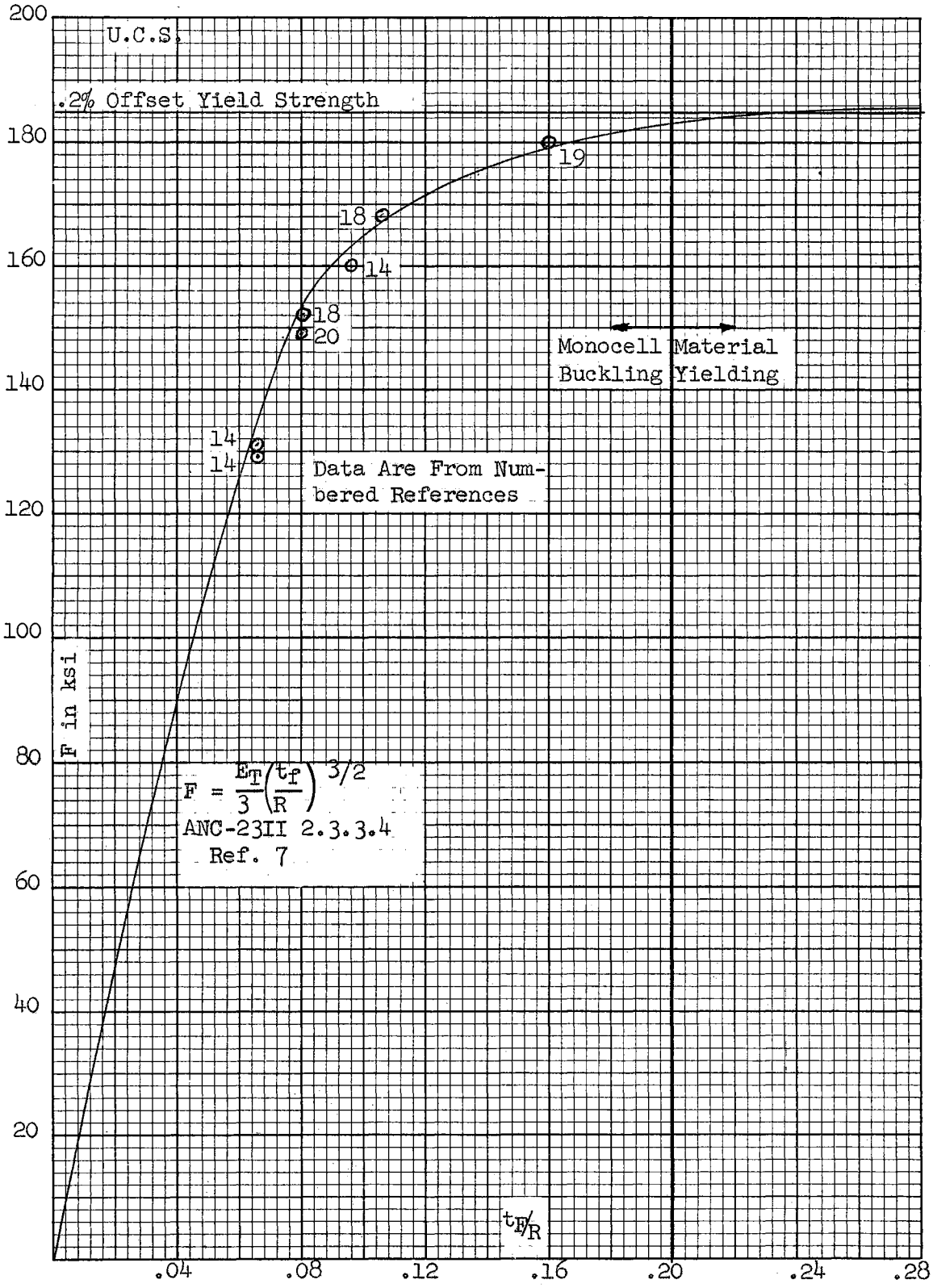

Figure 9. Comparison Between Predicted and Measured Monocell Buckling Stress for 17-7PH TH1050

assumed in this paper that monocell buckling is always avoided by adjusting the internal configuration of the core so that core density can be varied independently of face thickness without violating this rule of thumb.

Wrinkling The second mode of local instability is not nearly so well defined. Wrinkling in most of the literature is idealized as symmetrical, sine-shaped waviness of the faces. Two main types of theory exist, of which one (Ref.7, 4.7.1.1.3.2)depends heavily on knowledge of fabrication variables and the use of empirical constants. The other theory is much more convenient to use and is used herein.

This latter theory is developed in Reference 3 and 16, and the results are quoted in Reference 1 in the form

$F = k_w(E_R E_{zc} G_c)^{1/3}$ with the suggestion that a reasonable value of k_w might be .50. Theoretical values range from .78 to .961.

Using the results of previous paragraphs, the apparent core extensional modulus $E_{zc} = (d_c/477)E$; and the apparent core shear modulus $G_c = 10{,}000\ d_c$. Substituting these in the above equation gives the wrinkling stress as an implicit function of the core density alone, since E_R, whatever its form, is a function only of the stress level. In this paper it is assumed that $E_R = E_T$ is a suitable reduced modulus for face wrinkling. Then taking $E = 30 \times 10^6$ for steels,

$$F = 266{,}000 k_w (E_T/E)^{1/3} (d_c)^{2/3} \qquad \text{(EQ 4)}$$

This equation is plotted in Figure 10 for 17-7PH TH1050. It is apparent that the critical stress for wrinkling is above the yield strength of the material for core densities of less than 5 pcf if $K_w > .50$. Hence wrinkling should not occur in practical steel panels. The possibility, however, is discussed later.

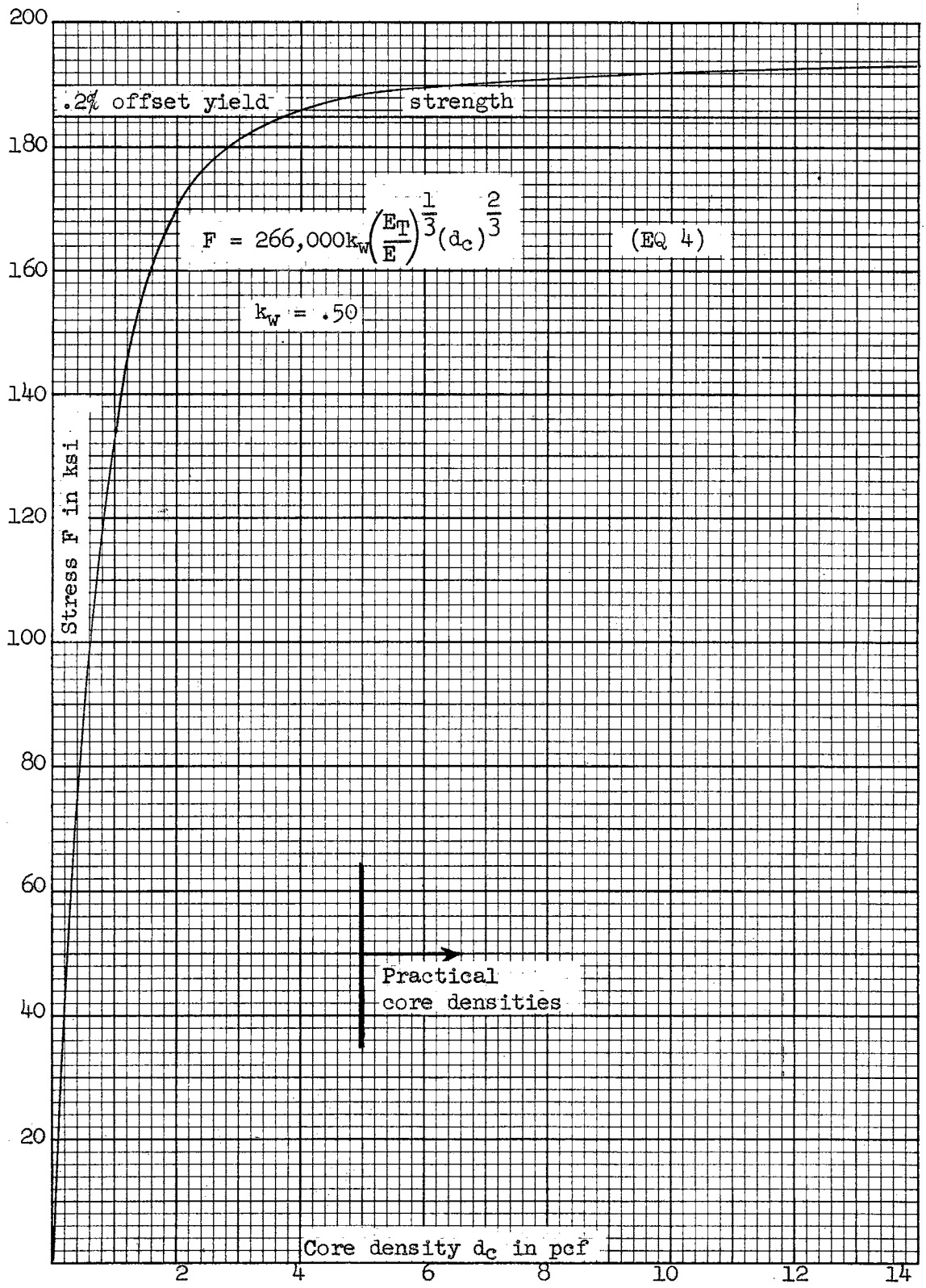

Figure 10. Predicted Wrinkling Stress for 17-7PH TH1050

CHAPTER III

THE OPTIMIZATION PROBLEM

Review of Previous Investigations.

The simplest approach to the problem of making the least weight of sandwich structure carry a given load is that given by Peery in Reference 21. He uses the Euler column formula, solves it for the face thickness, substitutes it in the expression for the weight of the column, and minimizes the column weight with respect to the core thickness. This procedure leads to the conclusion that for any load the most efficient column is one in which the core weighs twice as much as both faces together.

This procedure is open to several objections, among which are that the shear flexibility of the core, and the possibility of individual face instability are not accounted for. Besides which, as noted earlier, the basic unit of sandwich construction is the panel, not the column.

The approach used by Gerard in Chapter 6 of Reference 6 overcomes all these objections, and yields the same conclusion. However, other serious objections can be raised. In taking the derivative of solidity with respect to buckling stress, the core density, and panel buckling coefficient, and the secant modulus, are all considered as constants, effectively removing from consideration, core flexibility and plasticity effects. A less serious omission is the neglect of local face instability by simply showing that it will not ordinarily affect the

optimization analysis. As explained earlier, similar reasoning is employed in this paper, although with reservations due to lack of reliable face wrinkling data.

The work reported by Williams in Reference 3 includes both overall and local instability but draws no general conclusions as to optimum core weight. The overall instability expression used is a wide column formula similar to that given on page 21 , modified for edge support by a factor depending on the aspect ratio of the panel. This appears to describe a buckle pattern consisting of a single half-wave in each direction, which is of doubtful validity.

An excellent presentation is given by Flugge in Reference 2. Panel buckling is described by an expression similar to the one used herein, and face wrinkling by an expression similar to the thin panel formula of Yusuff (Ref. 16). The mathematical criterion for a maximum is employed. Wrinkling and buckling are permitted to occur simultaneously. (It is axiomatic in minimum weight analysis that two or more modes of failure should occur simultaneously (Ref. 6, para. 1.4). The only solid criticism of this approach is that it fails to account for plastic effects in the region of high stress. It is also difficult to compare different materials by this method due to the complexity of the parameters employed.

The best general approach appears to be that of Kaechele in Reference 1 which cannot be criticized on any of the points mentioned heretofore. The development is based on the panel buckling and wrinkling formulas given in this paper. The reduced modulus used is slightly different from the one used herein. The development is clearly explained, and the degree of straightforwardness lost in the approach is

compensated for in the convenience of the results which are in the form of charts. However much calculation is required to produce such charts for any given material. A minor criticism may be made that the criterion for comparing different materials, the 'equivalent stress', is a rather difficult concept, although fundamentally related to the stress/density and strength/weight ratios.

An approach nearly as good as that of Reference 1 is given in NACA TN 3751 (Ref. 4). However only the panel buckling mode is considered. The development is exceptionally straightforward but the parameters used are more complicated than those of this paper. No optimization is done during the development which is essentially a regrouping of the terms in the panel equation used in this paper.

Once the terms are grouped into independent parameters, the expression is plotted for reasonable ranges of these parameters, and relative efficiency is determined by inspection. Efficiency is not described by a particular ratio but is simply described by a relatively high value of a loading parameter occurring in conjunction with a relatively low value of a cross-sectional area parameter. Extensive calculation and plotting are required by this method.

A Simplified Approach

The first aspect of the problem is the choice of a criterion of efficiency. It is instructive to consider the simplest such criterion, the strength-to-weight ratio. This is simply the load a structure can support divided by the weight of the structure, both in pounds. For unstable structures this ratio takes the form $R = P_{cr}/W$ where P_{cr} is the critical (instability) load, and W is the weight of the structure.

For sandwich structure in compression,

$P_{cr} = F(2at_f)$

$W = W_f + W_c = (2abt_f d_f + abt_c d_c)/1728$, that is the weight of the faces plus the weight of the core, where dimensions are in inches and densities are in pcf. To be strictly correct, the weight of the braze alloy should be included in the sandwich weight, since none of it is lost in the fabricating process. However it is theoretically a constant increment for panels of the same area (ab), although in practice it may vary considerably, depending on whether it is deposited as a foil or as a paint, and on the gauge of the foil used. In any case it is not a large increment and is customarily neglected.

Another common structural efficiency criterion is the stress-to-density ratio, which for homogeneous materials may be written

$$A = F/d = \frac{P_{cr}/at}{W/abt} = \frac{P_{cr}b}{W} \text{ or in general } A = bR$$

Applying this result to sandwich material

$$A = bR = 1728bF(2at_f)/ab(2t_f d_f + t_c d_c) = \frac{1728F}{d_f + (t_c d_c/2t_f)}$$

In this expression the denominator is an 'effective' density of the sandwich, since, when multiplied by the load-carrying volume (of the faces), $2abt_f$, it gives the weight of the sandwich structure.

In Reference 22 this ratio is called the 'efficiency index'. It has several advantages over some other similar indices. It can be used to compare, directly, different materials. It can be expressed as a single-valued function of a structural parameter (the structural index) for a wide range of types of structure and modes of failure, and hence serves to compare different structural configurations as well as different materials.

However, when extended into the plastic region, any such index, including this one, becomes a function of the applied stress through the use of the reduced modulus described earlier, when applied to unstable structures. That is, the critical stress, F, depends on the reduced modulus, which is a function of the applied stress, f, which is equal to the critical stress at failure.

For this reason, it is not generally possible to solve instability type equations, including the panel buckling equation used herein, explicitly for the critical stress in the plastic region. Thus for computational purposes it is usually easiest to select a stress level, and with it a value of the reduced modulus, then calculate the structural variables which can associate with that stress.

Accordingly, the first step in the optimization process is to express the efficiency index 'A' in terms of a structural index (as yet undefined) and the stress level.

The panel buckling equation $F = \frac{K\pi^2 E_R}{4\lambda}\left(\frac{t_c + t_f}{a}\right)^2$ (EQ 3)

in which $K = 4/(1+V)^2$ may be written

$$V = \sqrt{\frac{\pi^2 E_R}{\lambda F}\left(\frac{t_c + t_f}{a}\right)^2} - 1 = M - 1 \qquad \text{(EQ 5)}$$

where M is simply a grouping symbol.

By definition $V = \frac{\pi^2 D}{a^2 U}$ from ANC-23 3.2.1.1 (Ref. 7) where D is the bending stiffness of the panel per inch of length, and U is shear stiffness per inch of length. Choosing simple expressions for these properties,

$$D = \frac{E_R t_f (t_c + t_f)^2}{2\lambda} \qquad \text{ANC-23 3.1.2(E)}$$

$$U = t_c G_c \qquad \text{ANC-23 3.1.3(A)}$$

and letting $G_c = kd_c$ for generality, where k = 10,000 psi/pcf for stainless steel honeycomb as noted on page 11 , there results

$$V = \frac{\pi^2 E_R t_f (t_c+t_f)^2}{2\lambda G_c t_c a^2} = \frac{t_f F M^2}{2k d_c t_c}$$

Setting the two expressions for V equal to each other,

$$V = M-1 = \frac{t_f F M^2}{2k d_c t_c} \quad \text{which upon rearranging gives}$$

$$(d_c t_c / 2t_f) = \frac{FM^2}{4k(M-1)} \qquad \text{(EQ 6)}$$

When this result is substituted in the previously derived expression for the efficiency index A, there results

$$A = \frac{1728F}{d_f + \frac{FM^2}{4k(M-1)}}$$

However since values of A from this expression tend to run around one million, it is convenient to omit the cubic feet-to-cubic inches conversion factor and write

$$A = \frac{F}{d_f + \frac{FM^2}{4k(M-1)}} \qquad \text{(EQ 7)}$$

This expression contains only F and M as variables. Since M contains only the variables F, E_R, and $\frac{a}{t_c+t_f}$ where E_R is a function of F only, then $\frac{a}{t_c+t_f}$ is the structural index for panel buckling and the efficiency index is now expressed in terms of the structural index and the stress level, which was desired.

It is noteworthy that considerable simplification has resulted from this manipulation. The variables d_c, G_c, b, and the thickness ratio $\frac{t_f}{t_c}$ have all been eliminated from the optimization problem which is now only three-dimensional. i.e. A, F, and $\frac{a}{t_c+t_f} = S$.

The straightforward application of mathematical maximizing criteria to Equation 7 yields (from Appendix A)

when $\partial A / \partial S = 0$, M = 2 which is elegantly simple,

when $\partial A / \partial F = 0$, $\frac{8kd_f}{F^2\left(\frac{E_R'}{E_R} - \frac{1}{F}\right)} = \left(\frac{M}{M-1}\right)^2 (M-2)$ (EQ A2) which is not difficult but is rather laborious to solve. The solution is also given in Appendix A.

From the form of Equation (7) it is apparent that if M=1, A=0. From Equation (5) if V=0, M=1. V=0 implies an infinitely stiff core which requires that the core be infinitely heavy since $G_c = kd_c$. Thus the condition M=1 implies an infinite core density which intuition indicates should result in zero efficiency by any criterion, confirming the results of Equation (7).

A point must now be considered which has not heretofore been mentioned. ANC-23 3.2.1.1 (Ref. 7) states that when V is greater than one (or $M > 2$ from Eq.5), Equation (3) no longer applies, and 'shear instability' buckling occurs. As will be shown later this is of academic interest only, but it affords some insight into the problem to show that the optimum structural index for a given stress level occurs along the boundary (M=2) between normal buckling and shear instability buckling which implies extremely light honeycomb cores.

In order to understand the results of the preceding comments it must be realized that, since $M = \sqrt{\frac{\pi^2 E_R}{\lambda F}\left(\frac{t_c+t_f}{a}\right)^2}$ Eq (8), from Equation 5, statements such as M=1 and M=2 are the equations for curves of stress versus structural index which produce certain behavior of the efficiency index and may also have other physical significance. Thus M=1 indicates a relationship between stress and structural index which will everywhere produce zero efficiency. It furthermore describes the highest stress level theoretically obtainable at each value of structural index since it implies a panel constructed with an (hypothetical) rigid core. M=2

indicates a relationship between stress and structural index such that the most efficient structural index for a given stress level is described. It also describes the limits of applicability of the normal panel buckling equation.

M may also be a function of F to produce certain desired variations of A. Equation A2 describes, although implicitly, the relationship between stress and structural index which produces the maximum efficiency for a given structural index.

In addition to producing desired variations of the efficiency index, by use of Equation 6 relationships between stress and structural index can be selected so as to produce desired variations of the ratio $(d_c t_c/2t_f)$, which contains the variables which were eliminated from the optimization process. In particular, it is possible to select a relationship between stress and structural index, say M=2, which defines the most efficient structural index for each stress level, by substitution in Equation 7 calculate the maximum efficiency obtainable at each stress level, and by substitution in Equation 6 define in general terms the structural and geometrical configurations of the most efficient panel constructions. It then remains only to apply the conditions of a particular problem to define completely, the optimum panel configuration for that problem. The foregoing generalities are best illustrated by some numerical examples.

Numerical Calculations

As noted earlier, for purposes of illustration, the high strength, high temperature stainless steel 17-7 PH TH 1050 is used throughout this paper. For this material d_f = 477 pcf, and k = 10,000 psi/pcf as pre-

viously shown. The necessary stress-strain information is given in Figure 6. For this material, as for most engineering materials, the value of Poisson's ratio in the plastic range may be taken as .50. Hence

$$\lambda = 1 - \mu^2 = 1 - .25 = .75$$

Table I gives the solutions of Equations (6) and (8) for various constant values of the parameter M. Table II gives the solutions of Equations (6) and (8) for the relationship of Equation A2. Table III gives the solution of Equation (7) for the useful ranges of structural index and stress. These tables are referenced internally in order to make them as nearly self-explanatory as possible. The ease and speed with which these tables can be constructed is particularly noteworthy. In order to obtain this simplicity in Table I, it is necessary to assume convenient values of F and M and plug them into Equations (6) and (8) to obtain the associated values of the construction parameter $(d_c t_c/2t_f)$ and the structural index, $S = \frac{a}{\sqrt{t_c+t_f}}$. Both equations are simple in form and well adapted to slide-rule calculation. As a matter of even greater convenience, once the solutions for M=1 have been found, the solutions for other values of M may be obtained by simple ratios.

Maximum utility of the information thus gained is obtained by plotting the contents of Tables I and II on a single chart, which, while it does not indicate values of efficiency does provide a large amount of information as to which ranges and combinations of structural index, stress level, and other configuration details will produce the most efficient panels. This is illustrated in Figure 11. Because of the simple form of Equation (7), it is usually not desirable to calculate Table III, but rather to calculate the efficiency index of

TABLE I

SOLUTIONS OF EQUATIONS 6 AND 8 FOR 17-7PH TH 1050

(EQ)	Operation	M	$Fx10^{-3}$	(1)	60	80	100	120	140	160	170	180	185	190	200
	Fig.6		$E_R x10^{-6}$	(2)	30.0	30.0	29.0	27.8	26.4	22.7	19.5	13.5	9.2	5.0	0
(8)		1.00	$\frac{a}{t_c+t_f}$	(3)	81.1	70.3	61.8	55.2	49.8	43.2	38.9	31.4	25.6	18.6	0
(8)	$\frac{(3)}{1.08}$	1.08	$\frac{a}{t_c+t_f}$	(4)	75.1	65.1	57.2	51.1	46.1	40.0	36.0	29.1	23.7	17.2	0
(6)	$\frac{(1)}{2743}$	1.08	$\frac{d_c t_c}{2t_f}$	(5)	21.9	29.2	36.5	43.8	51.1	58.4	62.0	65.7	67.5	69.4	73.0
(8)	$\frac{(3)}{1.09}$	1.09	$\frac{a}{t_c+t_f}$	(6)	74.4	64.5	56.7	50.6	45.7	39.6	35.7	28.8	23.5	17.1	0
(6)	$\frac{(1)}{3030}$	1.09	$\frac{d_c t_c}{2t_f}$	(7)	19.8	26.4	33.0	39.6	46.2	52.8	56.1	59.4	61.0	62.7	66.0
(8)	$\frac{(3)}{1.10}$	1.10	$\frac{a}{t_c+t_f}$	(8)	73.7	63.9	56.2	50.2	45.3	39.3	35.4	28.5	23.3	16.9	0
(6)	$\frac{(1)}{3306}$	1.10	$\frac{d_c t_c}{2t_f}$	(9)	18.1	24.2	30.2	36.2	42.3	48.3	51.3	54.4	55.9	57.4	60.4
(8)	$\frac{(3)}{1.20}$	1.20	$\frac{a}{t_c+t_f}$	(10)	67.6	58.6	51.5	46.0	41.5	36.0	32.4	26.2	21.3	15.5	0
(6)	$\frac{(1)}{5556}$	1.20	$\frac{d_c t_c}{2t_f}$	(11)	10.8	14.4	18.0	21.6	25.2	28.8	30.6	32.4	33.3	34.2	36.0
(8)	$\frac{(3)}{1.30}$	1.30	$\frac{a}{t_c+t_f}$	(12)	62.4	54.1	47.5	42.4	38.3	33.2	29.9	24.1	19.7	14.3	0
(6)	$\frac{(1)}{7101}$	1.30	$\frac{d_c t_c}{2t_f}$	(13)	8.5	11.3	14.1	16.9	19.7	22.6	24.0	25.4	26.1	26.8	28.2
(8)	$\frac{(3)}{1.60}$	1.60	$\frac{a}{t_c+t_f}$	(14)	50.7	43.9	38.6	34.5	31.1	27.0	24.3	19.6	16.0	11.6	0
(6)	$\frac{(1)}{9375}$	1.60	$\frac{d_c t_c}{2t_f}$	(15)	6.4	8.6	10.7	12.8	15.0	17.1	18.2	19.3	19.8	20.3	21.4
(8)	$\frac{(3)}{2.00}$	2.00	$\frac{a}{t_c+t_f}$	(16)	40.6	35.2	30.9	27.6	24.9	21.6	19.4	15.7	12.8	9.3	0
(6)	$\frac{(1)}{10000}$	2.00	$\frac{d_c t_c}{2t_f}$	(17)	6.0	8.0	10.0	12.0	14.0	16.0	17.0	18.0	18.5	19.0	20.0

TABLE II

SOLUTIONS OF EQUATIONS 6 AND 8 FOR OPTIMUM STRESS AND CONSTANT E, 17-7PH TH 1050

(EQ)	$Fx10^{-3}$	(1)	80	100	120	140	160	170	180	185	190	200
Fig.6	$E_R x10^{-6}$	(2)	30.0	29.0	27.8	26.4	22.7	19.5	13.5	9.2	5.0	0
(A2)	M^2	(3)	1.095	1.120	1.131	1.165	1.239	1.327	1.551	1.715	1.999	4.000
	M	(4)	1.046	1.058	1.063	1.079	1.113	1.152	1.245	1.310	1.414	2.000
(8)	$\frac{a}{t_c+t_f}$	(5)	67.2	58.4	51.9	46.2	38.8	33.8	25.2	19.5	13.2	0
(6)	$\frac{d_c t_c}{2t_f}$	(6)	47.6	48.3	53.9	51.6	43.9	37.1	28.5	25.6	22.9	20.0
	$Ex10^{-6}$	(7)	30.0	30.0	30.0	30.0	30.0	30.0	30.0	30.0	30.0	30.0
(8)	$\frac{a}{t_c+t_f}$	(8)	70.3	62.8	57.4	53.1	49.7	48.2	46.8	46.2	45.6	44.4

TABLE III

SOLUTIONS OF EQUATION 7 FOR 17-7PH TH 1050

Table Source	M	$Fx10^{-3}$	(1)	60	80	100	120	140	160	170	180	185	190	200
	1.00	A	(2)	0	0	0	0	0	0	0	0	0	0	0
I Row 5	1.08	A	(3)	120.3	158.0	194.7	230.4	265.1	298.8	315.4	331.7	339.8	347.7	363.6
I Row 7	1.09	A	(4)	120.7	158.9	196.1	232.3	267.6	302.0	318.9	335.6	343.9	352.0	368.3
I Row 9	1.10	A	(5)	121.2	159.6	197.2	233.8	269.6	304.6	321.8	338.7	347.2	355.5	372.2
I Row 11	1.20	A	(6)	123.0	162.8	202.0	240.7	278.8	316.3	334.9	353.4	362.5	371.7	389.9
I Row 13	1.30	A	(7)	123.6	163.8	203.6	243.0	281.9	320.3	339.3	358.3	367.7	377.1	395.9
I Row 15	1.60	A	(8)	124.1	164.7	205.0	245.0	284.6	323.8	343.3	362.7	372.4	382.1	401.3
I Row 17	2.00	A	(9)	124.2	164.9	205.3	245.4	285.1	324.5	344.1	363.6	373.4	383.1	402.4
II Row 6	EQ A2	A	(10)		152.5	190.4	226.0	264.9	307.2	330.7	356.1	368.1	380.1	402.4
$\frac{d_c t_c}{2t_f}$ =	0	A	(11)	125.8	167.7	209.6	251.6	293.5	335.4	356.4	377.4	387.8	398.3	419.3

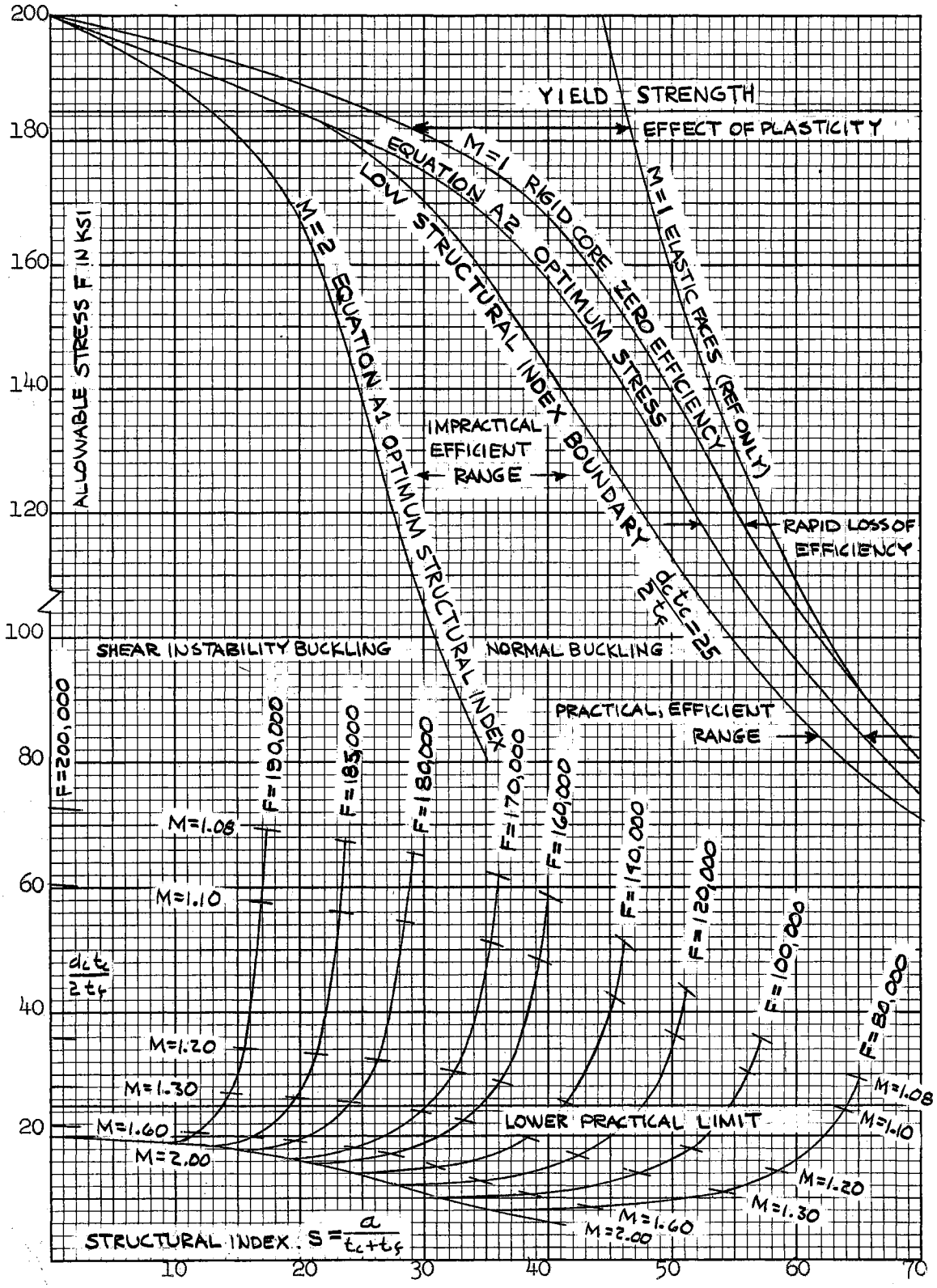

Figure 11. Design Chart for 17-7PH TH 1050 Panels

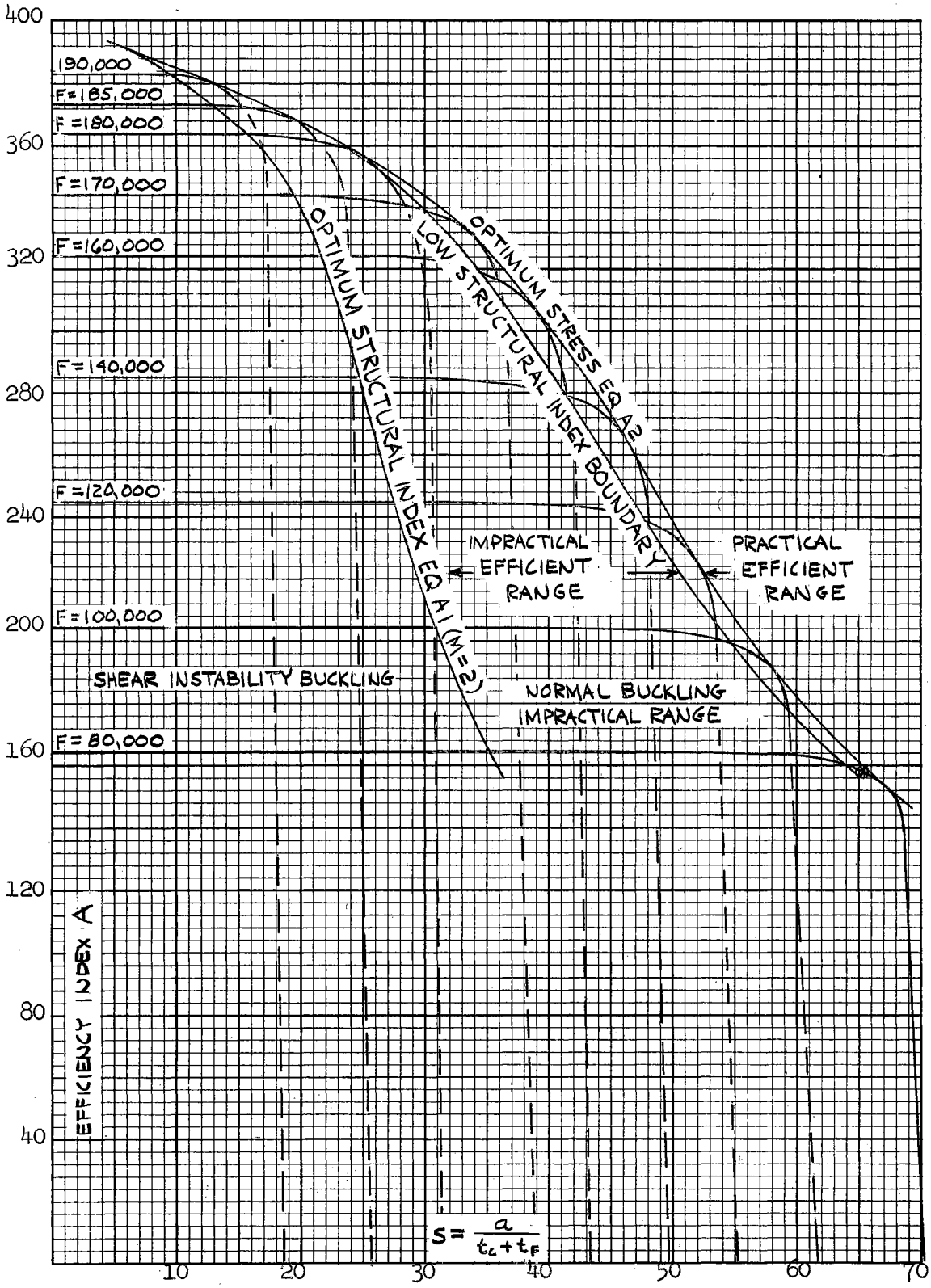

Figure 12. Efficiency Index vs. Structural Index

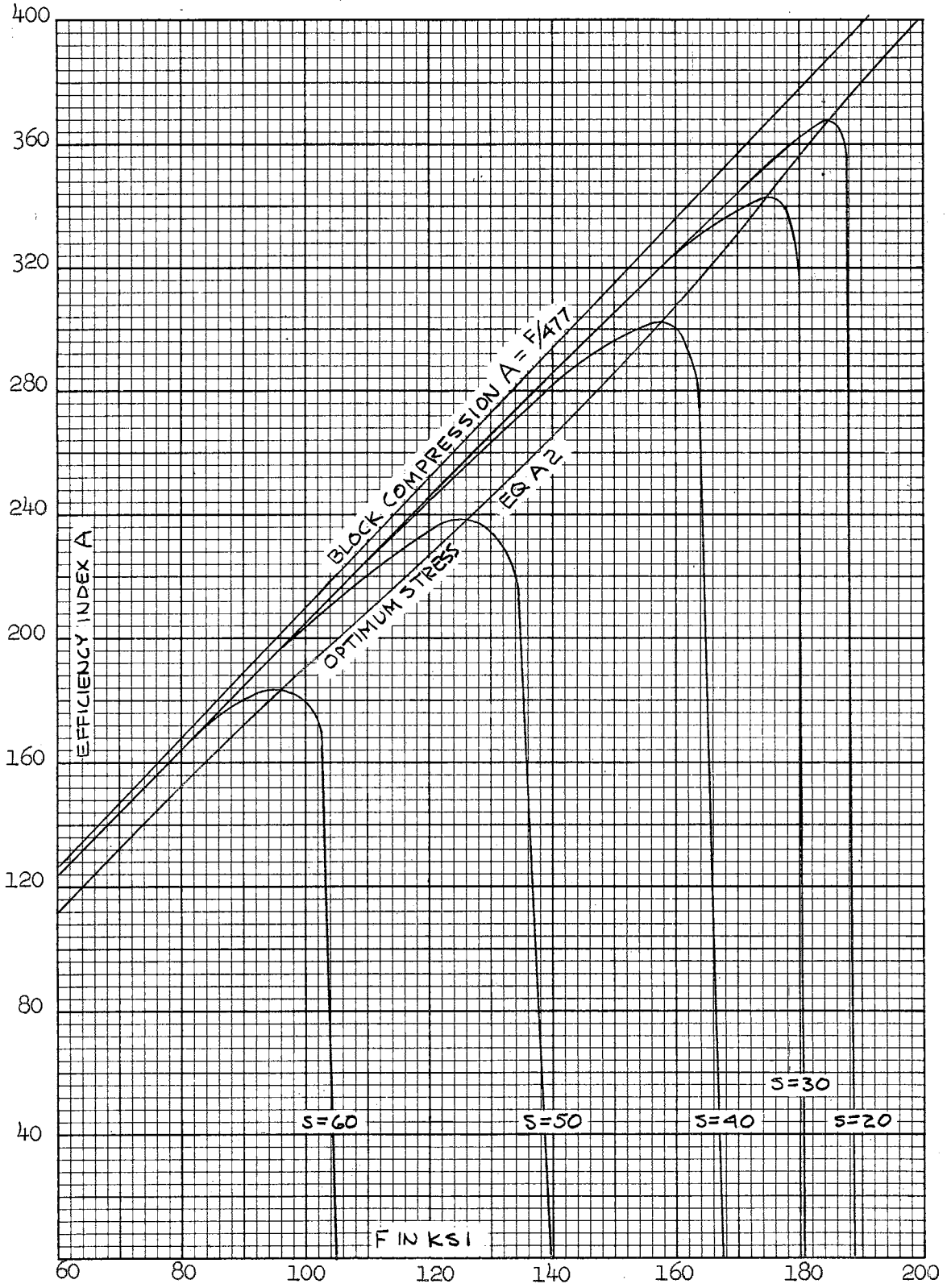

Fig. 13. Efficiency Index vs Stress Level

each panel which appears from Figure 11 to offer good efficiency. By this means a rather critical comparison can be made between panels of almost equal efficiency, and the effects of deviating slightly from optimum proportions may be narrowly appraised. This is an extremely desirable feature since it is quite possible that for some panel materials, as for the one considered herein, the ranges of truly optimum proportions and of practical construction simply do not overlap.

However for purposes of exposition, and providing additional insight, Table III has been calculated and the results plotted in Figure 12. As a means of further describing the three-dimensional surface generated by Equation (7), Figure 13 has also been presented, largely by cross-plotting from Figure 12.

The solutions of Equation (7) could logically and economically have been carried out in Tables I and II, by simply adding a row for this purpose below each row of solutions for Equation (6). As a typical example consider row (5) of Table I, which gives solutions for Equation (6) for various values of stress level, when M = 1.08. In the column for F=80,000 psi the value $(d_c t_c/2t_f) = 29.2$ pcf is given. Substituting in Equation (7), and using Equation (6), $A = \frac{F}{d_f + (d_c t_c/2t_f)} = \frac{80,000}{477+29.2} = 158.0$. This is the value given in Table III, and by taking the appropriate value of $\frac{a}{t_c+t_f} = 65.1$ from row (4) of Table I, this point may be plotted as in Figure 12. However, since the calculations in Tables I and II are fundamental, while the material in Table III is largely expository, these sets of calculations have been segregated in this paper.

Some discussion of Figures 11, 12, and 13 may prove illuminating. If, in accordance with the analogy used by Flugge in Reference 2, the

surface generated by Equation (7) is compared to a rise of ground (the 'A' hill), the upper part of Figure 11 may be described as a plan view or map, upon which might be drawn contour lines of constant efficiency index A.

Viewed from the South (Figure 12) the 'A' hill is an almost flat ramp-like surface, rising to the northward (increasing stress, F) and becoming narrower, with a very steep slope on the eastern flank. The line $\partial A/\partial S = 0$, i.e. M=2, locates the topological crest of the 'A' hill while the line $\partial A/\partial F = 0$ (EQ A2) locates the eastern military crest of the hill. The line A = 0, i.e. M=1, represents the foot of the eastern bluff as it intersects the base plane.

Figures 12 and 13 represent series of profiles cut through the hill, and viewed from the South and East, respectively.

For the purposes of design, it is sufficient to have derived only Figure 11. To employ another geological metaphor, it is of primary importance to define the boundaries within which it is profitable to 'prospect' for efficient panel configurations. In general, theoretical optima can only be approached in practice, due to the necessity of using standard material gauges, and other arbitrary restrictions.

Several purely practical considerations may be imposed on Figure 11 to further define the boundaries of efficient panel design. It has been found as a matter of practical hardware that is unwise to design for stress levels above the yield strength for these high-strength stainless steels. The extra care required in design and fabrication is simply not economically justifiable. This puts an upper limit on stress level in Figure 11.

Another practical limit may be derived from the following

considerations. Usual applications of honeycomb sandwich panels rarely require the face thickness t_f to be more than 10% of the core thickness t_c. In addition to this, it has been found that when the core density is below about 5 pcf, the honeycomb is so flexible and delicate that shop handling is difficult, and pressures used in the brazing process may damage it. These two factors combine to give a lower limit of the parameter, $\frac{d_c t_c}{2t_f}$, of $\frac{5}{2x.10} = 25$. If this limit is drawn on the lower part of Figure 11, and projected into the upper part, a 'low structural index' boundary is defined. That is, all practical panel configurations lie to the right of this line. For 17-7 PH TH 1050, Figure 11 shows that most of the efficient range lies to the left of this line, indicating the difficulty of designing truly optimum panels of this material.

Some further comments on Figure 11 may be useful. The field of stress level vs. structural index is divided by the line M=1, (V=0) into 'possible' and 'impossible' ranges. That is, any point to the right of this line represents a stress which cannot be withstood by a panel of that structural index. The 'possible' range is divided by the line M=2 (V=1.0) into 'shear instability' and 'normal' panel buckling ranges. The shear instability range is not of practical significance for most materials.

The normal buckling range is divided by the line $\partial A / \partial F = 0$ (Equation A2) into a range of very high efficiency, and a range in which efficiency falls off very rapidly as the line M=1 is approached. (This is because large increases in core density are required to produce even small increases in the critical stress near M=1.)

The normal buckling range is also divided into a 'practical'

range and an 'impractical' range of light cores and heavy faces by the line projected up from the line $\frac{d_c t_c}{2t_f} = 25$ in the lower part of the figure. For 17-7 PH TH 1050 the 'efficient' and 'practical' ranges do not overlap at 180,000 to 185,000 psi and do so only slightly at lower stresses. This may not be true for all materials, however.

It is noteworthy that the division into a very efficient range, and a range of sharply falling efficiency, is of rather slight utility, and for a large saving in labor with only a slight loss in convenience, Equation A2, and hence Table II, need not be calculated. As noted previously, it is not necessary to prepare Table III from Equation (7) either. The calculations are thus reduced to what must be nearly ultimate simplicity.

The Use of Figure 11

In the design problems considered herein it is assumed that the approximate size and shape of the panel to be defined are known or may be assumed. As in any design problem, it is assumed that the load which the panel must support without buckling, is known. (It is herein assumed that buckling constitutes failure, although actually the panel might continue to carry load even after buckling.)

One more 'open' variable needs to be filled by assumption before optimization may be begun. This is the stress level at which the panel should fail. This may seem odd at first glance, since it superficially appears that the higher the allowable stress, the higher the efficiency. However Figure 13 shows rather graphically that for a given structural index, stress level can profitably be raised only to the limit defined by Equation A2. Above this stress, efficiency falls off rapidly as

stress is increased. Then, it may be argued, why not use a structural index which permits the yield strength of the material to be obtained before buckling occurs? The answer is that at this point side conditions other than maximum strength/weight may be introduced.

As an example, consider an item of structure such as an airplane wing, the stiffness of which may be more important than its strength. It is quite possible that a wing could be designed for the design loads on a given airplane, such that, while it did not fail under those loads, it might deflect so far under normal flight loads as to compromise the performance of the airplane. The solution to this problem is simply to lower the stresses in the various structural elements of the wing, thus decreasing strains in these members, and lowering the cumulative deflections.

Other reasons for designing to a reduced stress level might be to inhibit material fatigue, or to maintain safe stress levels in areas of stress concentration and reduced area, such as rows of fasteners, although these are not normally considerations in design of compression structures.

Another more practical concern is the need in preliminary design to account, simply and quickly, for secondary loads and stresses. Provided that the secondary loads are not such as to reinforce the buckling pattern due to the primary loads, this may be handled by simply lowering the primary stress level by some 'guesstimated' margin.

With the preceding remarks as background, consider the following design problem: The loading intensity (total load divided by the total width) is 10,000 pounds per inch. The design stress has been fixed by other considerations, as 160,000 psi. End supports are 60 inches apart

and it is desired to examine the effects of dividing the total width into 20 inch panels. Then $P/a = 10{,}000$

$$P/2at_f = 160{,}000 = F$$

$$a = 20 \text{ and } b = 60$$

From the upper part of Figure 11 it may be seen that the structural index for any practical panel meeting these specifications must fall within the range $34.5 < S < 43.2$, and relatively efficient panels will be found only in the range $34.5 < S < 38.8$. For a first try assume $S = \frac{a}{t_c+t_f} = 34.5$. From the given conditions, $t_f = \frac{10{,}000}{2x160{,}000}$ $= .03125$ which is a standard gauge. Then since $S = \frac{a}{t_c+t_f} = \frac{20}{t_c+.03125}$ $= 34.5$, $t_c = \frac{20}{34.5} - .03125 = .55$. From the lower part of Figure 11, it is found that for $F = 160{,}000$ and $S = 34.5$, $\frac{d_c t_c}{2t_f} = 25.0$

$$\text{then } d_c = \frac{2x25xt_f}{t_c} = \frac{50x.03125}{.55} = 2.7 \text{ pcf.}$$

This is an impractically light core. The point to be noted is that while impractical points may sometimes be found to the right of the 'low structural index' boundary, no practical points will ever be found to the left of it.

For a second try assume $S = 38.8$. Then as before, $t_f = .03125$ and $t_c = \frac{20}{38.8} - .03125 = .484$. From the lower part of Figure 11, for $F = 160{,}000$ and $S = 38.8$, $\frac{d_c t_c}{2t_f} = 44.0$. Then $d_c = \frac{2x44x.03125}{.484} = 5.7$ pcf. This is a practical panel construction, and from Equations (6) and (7) $A = \frac{F}{d_f+(d_c t_c/2t_f)} = \frac{160{,}000}{477+44} = \frac{160{,}000}{521} = 307$. Furthermore, from a fundamental relationship given earlier, the weight of this panel is

$$W = \frac{2abt_f(d_f+d_c t_c/2t_f)}{1728} = \frac{2x20x60x.03125x521}{1728} = 22.6 \text{ lbs.}$$

For a slight further refinement, assume $S = 38.3$. By the preceding process, $t_f = .03125$, $t_c = .491$, $\frac{d_c t_c}{2t_f} = 39.5$, $d_c = 5.0$ pcf, $A = 310$, and $W = 22.4$ lbs. Within the assumptions of this paper, and neglect-

ing edge attachments, local reinforcements, if any, and braze alloy, this is the lightest panel which will fill the allotted space and carry the specified load.

In a real design problem, the designer might again divide the total width into panels of say, 24 inch width, and by the process illustrated above, converge upon the lightest panel of this width. He could then balance off the extra weight of the wider panels against the weight of the smaller number of edge supports required, to arrive at an optimum arrangement of his total structure. Such a problem is beyond the scope of this paper.

Summary and Conclusions

The selection of optimum proportions for a stainless steel panel is rendered difficult by three main considerations. One, there are several possible modes of failure; two, the range of useful stress levels is entirely above the proportional limit; and three, the critical buckling stress for these panels depends on a large number of panel physical properties.

In this paper, modes of failure other than panel buckling have been written off as not applicable to stainless steel panels with properly chosen core configurations. The non-rigorous but useful concept of a 'reduced' modulus is used to account for plasticity effects. The large number of structural variables in the panel buckling equation is reduced to a manageable number, first by selection of an efficiency criterion, the 'efficiency index', which for this particular case (and for some other loading cases) has the property of eliminating a number of panel variables from the optimization process.

The remaining variables are grouped into a 'structural index' and functions of the stress level. This leaves a three-dimensional optimization problem which is solved by a straightforward application of the usual processes of the differential calculus.

When the solutions are plotted, which is tremendously simplified by the introduction of the symbol 'M' in place of a group of variables, a chart results which, with the addition of some practical boundaries, serves to define the ranges within which practical, efficient panels may be designed.

This chart (Figure 11) relates all the panel variables, and in particular, shows those relationships which give high efficiency. Several conclusions can be drawn simply by inspection of this chart. For instance, if the chart is complete, it may be determined at a glance whether or not truly optimum panels can be designed within the limits of practical hardware.

It is also apparent from Figure 11 that, for 17-7PH TH 1050, truly optimum panels require honeycomb cores of impractically low density. This conclusion is in accord with those of NACA TN 3751 (Ref 4).

An interesting sidelight is also thrown on the problem by Figure 11. From the lower part of the figure it is apparent that the upper useful limit of the parameter $(d_c t_c/2t_f)$ does not exceed, say, 80 at the most. A little thought will show that if this expression is divided by the density of the face material, d_f = 477pcf, the resulting number is the ratio of the weight of the core to the weight of both faces. Here it is shown that the magnitude of this number does not exceed $\frac{80}{477}$ = .168 at most. This is at sharp variance with the conclusion reached in Reference 6 by simplified analysis that the weight of the core

should be twice the weight of both faces, and indicates the inadequacy of simplified analysis for sandwich structure.

A practical extension of this approach may be made into the high temperature ranges which may be of design interest for stainless steels. All that is required is that Fig. 6 be redrawn to reflect the tangent modulus variation of the stress-strain diagram of the material at the design temperature. The new data must be carried through Table I, at least, and will result in a new Figure 11. The upper limit of design stress in the new Fig. 11 should reflect the lowered yield strength at temperature.

It is quite possible that the question of wrinkling failure of the faces of a compression panel has been written off too lightly in this paper. However both RM 1895 (Ref. 1) and NACA TN 3751 (Ref. 4) avoided the question in the same way. It is probably fair to say that in the dim light of present knowledge, any attempt to include it in an analysis such as this would be shooting in the dark.

The most useful existing wrinkling theory now available (Ref. 16) can be reduced to relationships between the critical stress, the core density, and the thickness ratio (t_f/t_c). If, as the state of the art advances, these relationships can be retained, perhaps by the use of empirical coefficients, it appears possible to include wrinkling considerations as the panel configuration is evolved. Figure 11 contains the functions of these same variables which are associated with panel buckling. If the wrinkling relationships of these variables could be superimposed on the lower part of Figure 11, they could then be projected upward into the upper part of the figure and perhaps produce limitations on the choice of efficient compression sandwich panels. However this work must await the publication of sufficient wrinkling

test data to permit the evaluation of constants in the existing theories, or to indicate the need for a new theory.

REFERENCES

1. Kaechele, L. E. Minimum Weight Design of Sandwich Panels.RM 1895 U. S. Air Force Project Rand, 22 March 1957. ASTIA Document AD 133011

2. Flugge, W. The Optimum Problem of the Sandwich Plate. Journal of Applied Mechanics, March 1952.

3. Williams, D. Sandwich Construction, A Practical Approach for the Use of Designers. Great Britain Aeronautical Research Council R&M No. 2466 (NACA File No. N13037)

4. Johnson, Aldie E. Jr. and Joseph W. Semonian. A Study of the Efficiency of High-Strength, Steel, Cellular-Core Sandwich Plates in Compression. NACA TN 3751, 1956.

5. Hickman, William A. and Norris F. Dow. Direct Reading Design Charts for 75S-T6 Aluminum-Alloy Flat Compression Panels Having Longitudinal Extruded Z-Section Stiffeners. NACA TN 2435

6. Gerard, George. Minimum Weight Analysis of Compression Structures. 1956. New York University Press, Washington Square, New York.

7. Anon. Sandwich Construction for Aircraft Part II - Material Properties and Design Criteria. ANC-23, Air Force-Navy-Civil Subcommittee on Aircraft Design Criteria, Second Ed. 1955

8. Kelsey, Gellatly, and Clark. The Shear Modulus of Foil Honeycomb Cores. Aircraft Engineering Vol. XXX No. 356, Oct. 1958. (British Magazine. Available through the Institute of Aeronautical Sciences library service.)

9. Seide, Paul and Elbridge Z. Stowell. Elastic and Plastic Buckling of Simply Supported Solid-Core Sandwich Plates in Compression. NACA Rep. 967, 1950. (Supersedes NACA TN 1822, 1949.)

10. Gerard, George, and Herbert Becker. Handbook of Structural Stability Part I - Buckling of Flat Plates. NACA TN 3781, 1957

11. Stein, Bland A. Compressive Stress-Strain Properties of 17-7PH and AM 350 Stainless-Steel Sheet at Elevated Temperatures. NACA TN 4074, 1957

12. Stowell, Elbridge Z. A Unified Theory of Plastic Buckling of Columns and Plates. NACA Rep. No. 898, 1948

13. Anon. Precipitation Hardening Stainless Steels. Technical Data Manual, Armco Steel Corp. Middletown, Ohio.

14. Anon. Strength Data on All-Metal Honeycomb Sandwich Structure. Solar Aircraft Company, San Diego 12, California.

15. Norris, C. B. and W. J. Kommers. Short-Column Compressive Strength of Sandwich Constructions as Affected by the Size of the Cells of Honeycomb-Core Materials. Forest Products Laboratory Report No. 1817, 1950.

16. Yusuff, Syed. Theory of Wrinkling in Sandwich Construction. Journal of the Royal Aeronautical Society, Vol. 59, No. 529, Page 30, Jan. 1955.

17. Anon. Handbook of Adhesives. Bloomingdale Rubber Company. Aberdeen, Maryland.

18. Anon. Hi-Temp Sandwich Structure. Western Aviation Magazine. Nov. 1956. Occidental Publishing Co. 4328 Sunset Blvd. Los Angeles 29, Cal.

19. Anon. High Temperature Welded Honeycomb Core. Brochure N, June 1958. Swedlow Plastics Co. 6986 Bandini Blvd. Los Angeles 22, California.

20. Anon. Sandwich Structure - Summary of Characteristics and Mechanical Properties. Engineering Report 117R-29. Rohr Aircraft Corp. Chula Vista, California.

21. Peery, David J. Aircraft Structures, 1949. McGraw-Hill Book Company, Inc. New York, N.Y.

22. Schuette, E. H. and J. A. Gusack. The Structural Index - A Guide to Optimum Design. Condensed in Space/Aeronautics R&D Handbook, 1959-1960. Conover-Mast Publications Inc. 205 E. 42nd St. New York 17, N.Y.

23. Anon. Short Column Tests of Six Types of 'Squarcel' 17-7PH Steel Honeycomb Core Material in Sandwich. Laboratory Report 1741-4 dated Aug. 2, 1957. A. E. Zezula and Associated Metallurgical Engineers. 1334 East Slauson Ave., Los Angeles 11, California.

24. Anon. Tests Upon Six Types of 'Squarcel' 17-7PH Steel Honeycomb Core Material to Establish Their Respective Bare Compressive Strengths. Laboratory Report 1741-3. A. E. Zezula and Associated Metallurgical Engineers. 1334 East Slauson Ave., Los Angeles 11, California.

25. Anon. Design Guide for Brazed Stainless Steel Sandwich Aeronca Manufacturing Corp. Middleton, Ohio.

26. Anon. Core Material: Corrosion and Heat Resisting Steel Honeycomb Specification. Dated Nov. 1956. John J. Foster Manufacturing Co., Santa Ana, California.

27. Anon. 17-7PH Core Material Comparison Data Sheet. Dated June 12, 1958. John J. Foster Manufacturing Co. Santa Ana, California.

28. Anon. ARTC-17 Test Procedures for High Temperature Sandwich Structure. Aircraft Industries Association report dated June 15, 1958. AIA Technical Service, 7660 Beverly Blvd. Los Angeles 36, California.

29. Cathers, R. T. and R. V. Claflin. Literature Survey of Sandwich Construction. Engineering Report LB 25606 dated Nov. 30, 1957. Douglas Aircraft Co. Long Beach, California.

APPENDIX A

Introduction

Equation (7) has been presented in terms of the parameter M because of the resulting simplicity in numerical computations. Because of the cumbersome form of Equation (7) if the expression M (Equation 8) is substituted in it, it is convenient to retain the variable, M. By this device the necessary algebra is greatly simplified, while the partial differentiation is made slightly more difficult. Because of the uncomplicated nature of the surface generated by Equation (7), it is sufficient simply to set the partial derivatives of A with respect to S and F equal to zero, to obtain optimum relationships between S and F. In the following operations the symbol M' will be used to denote the partial of M with respect to whichever independent variable is being considered.

Partial Differentiation With Respect to Structural Index

$$A = \frac{F}{d_f + \frac{FM^2}{4k(m-1)}} = \frac{4kF(M-1)}{4kd_f(M-1)+FM^2} \qquad \text{Equation (7)}$$

$$\partial A/\partial S = 0 = \left[4kd_f(M-1)+FM^2\right] 4kFM' - 4kF(M-1)\left[4kd_fM' + 2FMM'\right]$$

$$4kd_fMx4kFM' - 4kd_f \times 4kFM' + 4kF^2M^2M' - 4kFM \times 4kd_fM' + 4kF \times 4kd_fM'$$

$$- 4kFM \times 2FMM' + 4kF \times 2FMM' = 0$$

$$16k^2Fd_fMM' - 16k^2Fd_fM' + 4kF^2M^2M' - 16k^2Fd_fMM' + 16k^2Fd_fM' - 8kF^2M^2M'$$

$$+ 8kF^2MM' = 0$$

$$4kF^2M^2M' = 8kF^2MM'$$

$$M = 2 \qquad \text{Equation (A1)}$$

Partial Differentiation With Respect to Stress Level

$$A = \frac{4kF(M-1)}{4kd_f(M-1)+FM^2} \qquad \text{Equation (7)}$$

$$\partial A/\partial F = 0 = \left[4kd_f(M-1)+FM^2\right]\left[4kFM'+4k(M-1)\right] - \left[4kF(M-1)\right]\left[4kd_fM'+2FMM'+M^2\right]$$

$$\left[4kd_fM - 4kd_f + FM^2\right]\left[FM'+M-1\right] - \left[FM-F\right]\left[4kd_fM'+2FMM'+M^2\right] = 0$$

Expanding this;

$$4kd_fFMM' + 4kd_fM^2 - 4kd_fM - 4kd_fFM' - 4kd_fM + 4kd_f + F^2M^2M' + FM^3 - FM^2$$

$$= 4kd_fFMM' - 4kd_fFM' + 2F^2M^2M' - 2F^2MM' + FM^3 - FM^2$$

Collecting like terms;

$$4kd_fM^2 - 8kd_fM + 4kd_f - F^2M^2M' + 2F^2MM' = 0$$

$$4kd_f(M^2 - 2M + 1) + M'(-F^2M^2 + 2F^2M) = 0$$

$$4kd_f(M-1)^2 = F^2M(M-2)M' \quad \text{where, since } M = \left(\frac{\pi^2E_R}{\lambda FS^2}\right)^{\frac{1}{2}} \qquad \text{EQ (8)}$$

$$M' = \partial M/\partial F = \frac{1}{2}\left(\frac{\lambda FS^2}{\pi^2E_R}\right)^{\frac{1}{2}}\left(\frac{\lambda FS^2\pi^2E_R' - \pi^2E_R\,S^2}{\lambda^2F^2S^4}\right)$$

$$= \frac{1}{2}\left(\frac{\lambda FS^2}{\pi^2E_R}\right)^{\frac{1}{2}}\left(\frac{\pi^2E_R}{\lambda FS^2}\right)\left(\frac{E_R'}{E_R} - \frac{1}{F}\right)$$

$$= \frac{M}{2}\left(\frac{E_R'}{E_R} - \frac{1}{F}\right) \qquad \text{where } E_R' = dE_R/dF$$

Hence

$$4kd_f(M-1)^2 = F^2M(M-2)\,\frac{M}{2}\left(\frac{E_R'}{E_R} - \frac{1}{F}\right)$$

and, by re-arranging

$$\frac{8kd_f}{F^2\left(\frac{E_R'}{E_R} - \frac{1}{F}\right)} = \left(\frac{M}{M-1}\right)^2 (M-2) \qquad \text{Equation (A2)}$$

This is the condition for the optimum stress level for each value of structural index. It is still in terms of the parameter M, which has now served its purpose.

The problem of eliminating M is best handled in two steps. The first is to determine M as a function of F. This is most readily accomplished by calculating the value of the left-hand side of the equation for a number of values of stress, F. The values of M which make the right-hand side of the equation equal to these left-hand values may be read from a plot of the right-hand side as in Figure 14. This gives pairs of values of F and M which satisfy Equation A2.

The second step is simply to substitute these simultaneous pairs into Equation (8) to obtain a set of pairs of values of F and S $= \frac{a}{t_c+t_f}$ which satisfy the equation.

The first step is carried out in Tables IV and V, and in Figure 14. The results are given in row (3) of Table II, and the second step is carried out in rows (4), (5), and (6) of Table II.

A few observations may be made from the form of Equation (A2), which will simplify the necessary calculations. Since E_R' is always negative, the left-hand side of the equation is always negative. From the form of the right-hand side, it can only be negative for values of M less than 2.0. The curve of the right-hand side obviously passes through zero at M=0 and M=2, and is discontinuous at M=1. From Figure 11, it is apparent that values of M less than 1.0 are without physical meaning in this problem, so that it necessarily follows that only the branch of the curve of the right-hand side lying between M=1 and M=2 is of interest.

As a matter of practical draftsmanship, it is just as easy to plot the right-hand side against M^2 as against M, and the accuracy of reading the plot is improved by this device. For this reason, Figure 14 is plotted with M^2 as the abcissa.

As elsewhere in this paper, calculations are carried out for 17-7PH TH 1050, for which k = 10,000, d_f is 477 pcf, and the stress-strain data is given in Figure 6.

TABLE IV

$$\text{Solution of } X = \frac{8kd_f}{F^2\left(\frac{E_R'}{E_R} - \frac{1}{F}\right)} = \frac{8\times10{,}000\times477}{F^2\left(\frac{E_R'}{E_R} - \frac{1}{F}\right)} = \frac{38.160}{\left(\frac{F}{1000}\right)^2\left(\frac{E_R'}{E_R} - \frac{1}{F}\right)} \quad *$$

Source	Operation												
Fig. 6		(1)	$F \times 10^{-3}$	80	100	120	140	160	170	180	185	190	200
Fig. 6		(2)	$E_R \times 10^{-6}$	30.0	29.0	27.8	26.4	22.7	19.5	13.5	9.2	5.0	0
	(3)/(2)	(3)	E_R'	0	- 66	- 46	-114	-247	-416	-745	-789	-745	-315
	1000/(1)	(4)	$\frac{E_R'}{E_R} \times 10^{-6}$	0	-2.276	-1.655	-4.318	-10.88	-21.33	-55.18	-85.76	-149.0	
	(4)-(5)	(5)	$\frac{1}{F} \times 10^{-6}$	12.50	10.00	8.333	7.143	6.25	5.88	5.56	5.40	5.3	
	$\frac{38.160^*}{(1)^2 \times (6)}$	(6)		-12.50	-12.28	-9.99	-11.46	-17.13	-27.21	-60.74	-91.16	-154.3	
		(7)	X	-477.0	-310.8	-265.3	-169.9	-87.01	-48.52	-19.39	-12.23	-6.85	

TABLE V

Solution of $X = \left| \frac{M}{M - 1} \right|^2 (M - 2)$

M	M - 1	M - 2	X	M^2
1.045	.045	-.955	- 515.0	1.092
1.050	.050	-.950	- 419.0	1.102
1.060	.060	-.940	- 293.4	1.124
1.070	.070	-.930	- 217.3	1.145
1.090	.090	-.910	- 133.5	1.188
1.100	.100	-.900	- 108.9	1.210
1.130	.130	-.870	- 65.7	1.277
1.150	.150	-.850	- 50.0	1.322
1.170	.170	-.830	- 39.3	1.369
1.200	.200	-.800	- 28.8	1.440
1.220	.220	-.780	- 24.0	1.488
1.250	.250	-.750	- 18.8	1.562
1.300	.300	-.700	- 13.1	1.690
1.350	.350	-.650	- 9.67	1.822
1.400	.400	-.600	- 7.35	1.960
1.414	.414	-.586	- 6.84	2.000
1.600	.600	-.400	- 2.85	2.560
1.800	.800	-.200	- 1.01	3.240
2.000	1.000	0	0	4.000

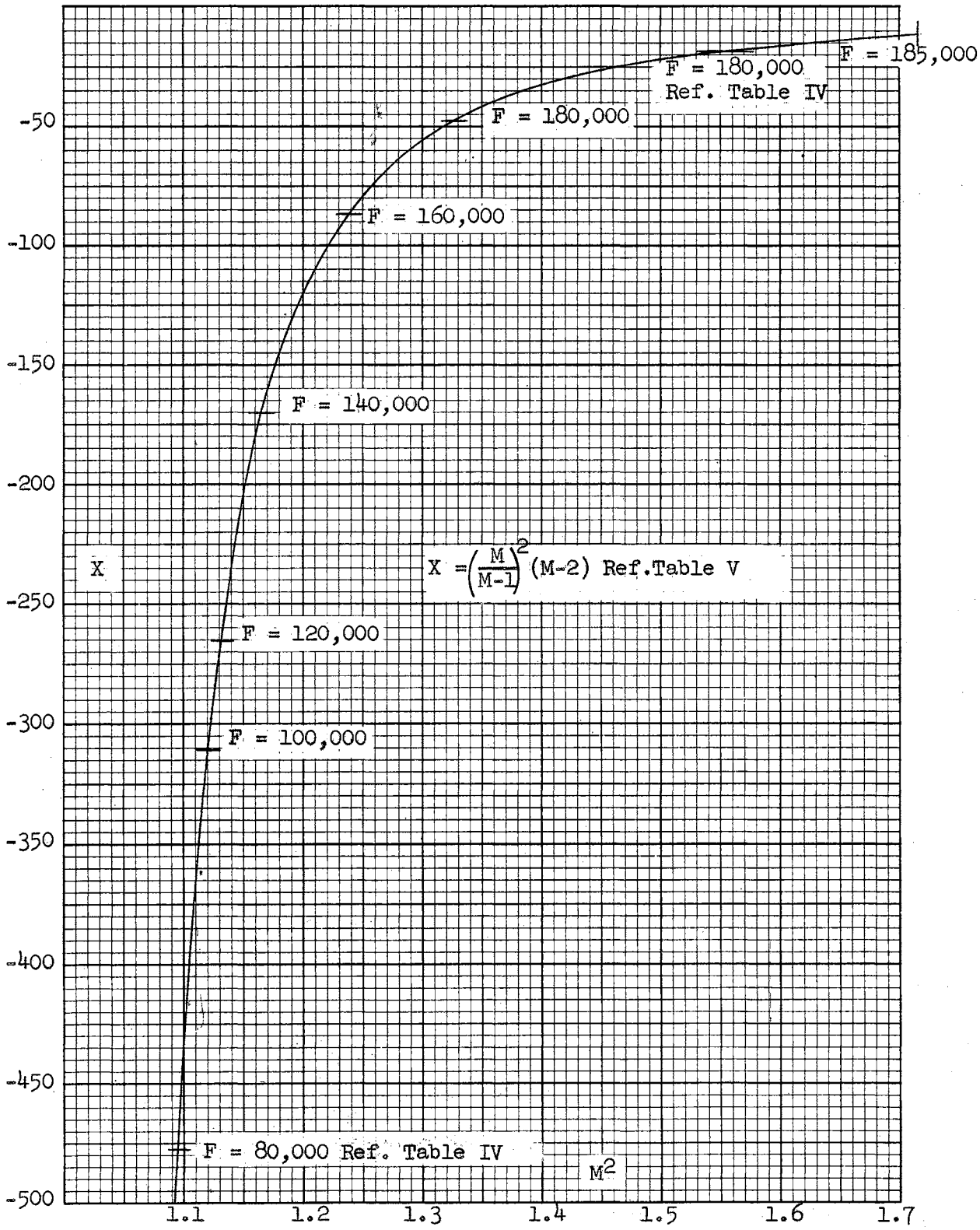

Figure 14. Plot of the Right-hand Side of Equation A2

LIST OF SYMBOLS

DIMENSIONS

a = length of the loaded edges of the panel.

b = length of the unloaded edges of the panel.

t = total thickness of a sandwich or homogeneous panel.

t_c = thickness of the honeycomb core.

t_f = thickness of one face of a sandwich panel. Both faces assumed equally thick.

D = diameter of a circle inscribed in a nominal honeycomb cell.

R = radius of a circle inscribed in a nominal honeycomb cell.

t_r = thickness (gauge) of ribbon or foil used in fabricating honeycomb core.

L = effective length of a column.

ρ = radius of gyration of a column = $\frac{t_c+t_f}{2}$ for sandwich columns.

PANEL PROPERTIES

S = structural index = $\frac{a}{t_c+t_f}$ for panel buckling.

$\frac{t_f}{t_c}$ = sandwich thickness ratio.

$\frac{a}{b}$ = panel aspect ratio.

d_c = weight density of honeycomb core in pounds per cubic foot (pcf).

E_{cz} = core extensional modulus in the out-of-plane direction.

G_{cxz} = apparent core shear modulus in the x (ribbon) direction.

G_{cyz} = apparent core shear modulus in the y (cross-ribbon) direction.

G_c = 'effective' apparent core shear modulus.

W = weight of panel or panel component.

I = area moment of inertia of a cross-section of a sandwich column or panel.

D = bending stiffness per inch of cross-section = $\frac{E_R t_f (t_c+t_f)^2}{2}$

U = shear stiffness per inch of cross-section = $t_c G_c$.

$V = \frac{\pi^2 D}{a^2 U}$

K = panel buckling coefficient = $\frac{4}{(1+V)^2}$ for sandwich panels.

M = a grouping symbol representing $\left[\frac{\pi^2 E_R}{\lambda F}\left(\frac{t_c+t_f}{a}\right)^2\right]^{\frac{1}{2}}$

M' = partial derivative of M with respect to F or S.

X = a symbol representing the value of either side of Equation (A2).

CONSTANTS

k = the ratio of 'effective' apparent core shear modulus to core density = 10,000 psi/pcf for 17-7PH TH1050.

k_w = a theoretical constant in the sandwich wrinkling expression, Equation (4) which possibly should have a lower, empirical, value.

LOADS AND STRESSES

P_{cr} = critical buckling load for columns or panels.

P_E = critical column buckling load if core shear flexibility is neglected; $= \frac{\pi^2 E_R I}{(L)^2}$

P_s = shear instability load, = $at_c G_c$.

F = critical instability stress for any mode of failure.

f = applied stress.

EFFICIENCY CRITERIA

R = strength-to-weight ratio.

A = critical stress-to-density ratio, and called 'efficiency index'.

MATERIAL PROPERTIES

E = Young's modulus

G = modulus of rigidity = $\frac{E}{2(1+\mu)}$

E_T = tangent modulus

E_R = reduced modulus

E_R' = derivative of reduced modulus with respect to stress.

F_{cy} = compressive yield strength.

F_{cu} = ultimate compressive strength.

d = weight density.

μ = Poisson's ratio. It is assumed that $\mu_e = .30$, and $\mu_p = .50$.

$\lambda = (1 - \mu^2)$

SUBSCRIPTS

c = core

E = Euler

e = elastic

f = faces

p = plastic

R = reduced

T = tangent

w = wrinkling

x = core ribbon direction

y = core cross-ribbon direction

z = out-of-panel-plane direction

VITA

William Cromer Burkitt

Candidate for the Degree of

Master of Science

Thesis: A SIMPLIFIED APPROACH TO THE OPTIMIZATION OF STAINLESS STEEL HONEYCOMB SANDWICH IN COMPRESSION

Major Field: Aircraft and Civil Engineering

Biographical:

Personal Data: Born in Lincoln, Nebraska, May 18, 1925, the son of Joel L. and Norma Marie Burkitt.

Education: Attended grade school in Tulsa, Oklahoma; graduated from Tulsa Central High School in 1942; received the Bachelor of Science degree in Aeronautical Engineering from the University of Tulsa in May, 1948; took Graduate courses in mathematics at the University of Wichita, in Wichita, Kansas in 1949, and 1950; completed requirements for the Master of Science degree in May, 1960.

Professional experience: Employed by Boeing Airplane Company of Wichita, Kansas as draftsman, checker, liaison engineer, and stress analyst, for seven years; employed in 1955 by Douglas Aircraft Company, Tulsa, Oklahoma as stress analyst and lead engineer; is now a structures engineer and lead engineer in the Strength Group of the Engineering department.

Professional organizations: Is a Member of the Institute of Aeronautical Sciences.